Climate velocity and the future global redistribution of marine biodiversity

Molinos, Jorge Garcia; Halpern, Benjamin S; Schoeman, David S; et.al.

Molinos, J. G., Halpern, B. S., Schoeman, D. S., Brown, C. J., Kiessling, W., Moore, P. J., Pandolfi, J. M., Poloczanska, E. S., Richardson, A. J., & Burrows, M. T. (2016). Climate velocity and the future global redistribution of marine biodiversity. Nature Climate Change, 6, 83–88.
https://doi.org/10.1038/nclimate2769
Document Type: Accepted Version

Link to Published Version: https://doi.org/10.1038/nclimate2769

Climate velocity and the future global redistribution of marine biodiversity

Jorge García Molinos[1,2*], Benjamin S. Halpern[3,4], David S. Schoeman[5], Christopher J. Brown[6], Wolfgang Kiessling[7,8], Pippa J. Moore[9,10], John M. Pandolfi[11], Elvira S. Poloczanska[12], Anthony J. Richardson[12,13] and Michael T. Burrows[1]

[1]Scottish Association for Marine Science, Oban, Argyll PA37 1QA, UK. [2]National Institute for Environmental Studies, 16-2 Onogawa, Tsukuba, Ibaraki 305-8506, Japan. [3]Bren School of Environmental Science and Management, University of California, Santa Barbara, California 93106, USA. [4]Imperial College London, Silwood Park Campus, Buckhurst Road, Ascot SL5 7PY, UK. [5]School of Science and Engineering, University of the Sunshine Coast, Maroochydore, Queensland QLD 4558, Australia. [6]The Global Change Institute, University of Queensland, Brisbane, Queensland 4072, Australia. [7]GeoZentrum Nordbayern, Paläoumwelt, Universität Erlangen-Nürnberg, Loewenichstrasse 28, 91054 Erlangen, Germany. [8]Museum für Naturkunde, Invalidenstrasse 43, 10115 Berlin, Germany. [9]Institute of Biological, Environmental and Rural Sciences, Aberystwyth University, Aberystwyth SY23 3DA, UK. [10]Centre for Marine Ecosystems Research, Edith Cowan University, Perth 6027, Australia. [11]School of Biological Sciences, Australian Research Council Centre of Excellence for Coral Reef Studies, The University of Queensland, Brisbane, Queensland 4072, Australia. [12]CSIRO Oceans and Atmosphere Flagship, Ecosciences Precinct, Boggo Road, Brisbane, Queensland 4001, Australia. [13]Centre for Applications in Natural Resource Mathematics (CARM), School of Mathematics and Physics, The University of Queensland, St Lucia, Queensland 4072, Australia.

*Corresponding author: Jorge.Garcia-Molinos@sams.ac.uk

Anticipating the effect of climate change on biodiversity, in particular changes in community composition (i.e., beta-diversity), is crucial for adaptive conservation management[1], but remains a critical gap[2]. Here, we use climate-velocity trajectories[3], together with information on depth preferences, coastal affinity, and thermal tolerances, to project changes in global patterns of marine species richness and for the first time community composition under the IPCC Representative Concentration Pathways[4] (RCPs) 4.5 and 8.5. Our simple, intuitive approach emphasizes climate connectivity, and enables us to model over 12 times more species than previous studies[5, 6]. We find that range expansions prevail over contractions for both RCPs up to 2100, producing a net global increase in richness and temporal changes in composition driven by the redistribution rather than the loss of diversity. Conversely, widespread invasions homogenize present-day communities across multiple regions. High extirpation rates are expected regionally (e.g., Central Indo-Pacific), particularly under RCP8.5, leading to strong decreases in richness and the anticipated formation of no-analogue communities via species turnover where invasions are common. The spatial congruence of these patterns with contemporary human impacts[7] highlights potential areas of future conservation concern. These results suggest strongly that the millennial stability of current global marine diversity patterns, against which conservation plans are assessed, will change rapidly over the course of the century in response to ocean warming.

Climate change is expected to become the greatest driver of change in global biodiversity in the coming decades[8]. To avoid extinction, organisms exposed to a changing climate can respond by adapting to the new conditions within their current range or by dynamically tracking their climatic niches in space (distribution shifts) or time (phenological shifts).

Although the evolutionary potential for marine organisms to cope with climate change remains uncertain[9], distribution shifts are already widely observed[10, 11, 12] and likely to become increasingly important given the expected intensification of current rates of climate change[13].

Forecasting climate-driven distribution shifts is challenging because they depart frequently from expected patterns of simple poleward movement[12]. However, recent evidence suggests that local climate velocity[14], a measure of the speed and direction of migrating isotherms, is a useful and simple predictor of the rate and direction of shift across a wide variety of marine taxa[10, 11, 15]. Here we use trajectories of climate velocity[3] to predict global marine biodiversity patterns at 1°-resolution under future anthropogenic climate change. Previous attempts to project climate impact on species distributions[5, 6, 16] have all been based on the same bioclimatic-niche and population-dynamics model developed by Cheung et al.[5]. These are limited to sufficiently well-studied, commercially exploited species, and focus on changes in species richness. Our simple, intuitive model allows us instead to model over 12 times more species spanning a wide range of taxonomic groups (12,796 marine species from 23 phyla; Supplementary Table S1). Importantly, our analysis is not limited to changes in species richness but, for the first time at a global scale, looks into the effect of climate change on spatio-temporal patterns in community composition, that is, beta diversity (see Methods). Because beta-diversity quantifies the rate of change in species in space or time, as opposed to the diversity of species within a community, it can provide crucial insights into the effects of environmental change, including climate change, on biodiversity[17]. Finally, to contextualize our projections to current conservation pressures, we explore the spatial congruence between future anthropogenic climate change impacts, as suggested by our projections, and the degree of contemporary human impacts on the ocean[7].

Based on modelled distribution data[18], we projected shifts in current thermal niche space for each taxon by calculating the trajectory that isotherms will follow up to 2100 based on RCPs 4.5 and 8.5 (Table S2 and Fig. S1), integrating through time the spatial variation in the magnitude and direction of local climate velocities (see Methods and Fig. S2). Occupancy within the new domain was determined thereafter as a function of thermal and habitat suitability, in terms of depth and coastal affinity, for each species (Figs S3-S4). Global warming nevertheless represents a very distinctive fingerprint of climate change on our oceans, unequivocally linked to species distribution shifts[10, 11]. Our analysis thus provides the simplest expectation for the future redistribution of biodiversity (i.e., ocean surface warming is the only driver of change to which species respond by shifting their distributions). Our projections of range shifts refer exclusively to those expected in response to changes in mean sea surface temperature and should therefore be interpreted with this caveat in mind (see Supplementary Material for a detailed discussion on the assumptions and uncertainties associated with our model). The outcome of climate change on biodiversity will depend on many abiotic and biotic factors, as well as on direct human impacts, besides global warming.

Our model predicts strong changes in present-day species richness (Fig. 1a), with contrasting outcomes between climate-change scenarios and considerable regional variability (Figs 1b, c and S5). These results are in general agreement with previously predicted patterns[5, 6], highlighting the pivotal role of temperature on species distribution shifts and supporting the adequacy of our model. Though similar in the short-term (Fig. S5), patterns of invasion and extirpation under both RCPs clearly diverge in mid-century (2040-2065), which under the RCP8.5 is a period of transition from a prevailing net gain to a net loss of biodiversity. Overall, projections from RCP8.5 (2006-2100) show a symmetrical latitudinal peak in net richness gain at ~20° N-S, and widespread areas of richness loss near the equator, concentrated in the Central Indo-Pacific (Fig. 1c). This pattern is consistent with that inferred from paleontological records during past episodes of rapid climate warming[19]. High rates of extirpation are expected for equatorial species under moderate warming (2-3 °C)[20] because their thermal tolerance breadth reflects the low variability in temperature within their ranges, while their capacity for acclimatization is comparatively lower[21]. Despite general spatial patterns remained unaltered (see Supplementary Methods and Fig. S6), extirpations, but not invasions, were highly sensitive to the criteria used to define the upper thermal tolerances of species, which stresses the importance of this parameter and the narrow temperature margin associated with local extinctions. In contrast, net losses under the RCP4.5 are projected to be low by 2100 (Fig. 1b), with the symmetrical latitudinal peak in richness located at lower latitudes (~10° N-S; Fig. 1b); a pattern resulting from the overriding effect of species invasions relative to local extinctions (Fig. S5).

Changes in composition of present communities are projected to be large by 2100 across the Arctic, the Central Indo-Pacific, the 10-20° N-S latitudinal bands and the Southern Ocean (Fig. 2 a, b). Changes are more intense and widespread under RCP8.5 (Fig. 2b) than RCP4.5 (Fig. 2a), mainly driven by the invasion of species into local communities without loss of resident species (i.e., nestedness; Fig. 2e) and, in subtropical areas and the Southern Ocean, temporal turnover (i.e., species replacement; Fig. 2c). Recent evidence suggests that the systematic loss of species is not a global driver of the temporal change in community composition of present-day communities[2]; we predict this will hold into the future. Although extinctions are projected to be regionally important (Fig. S5), it is their combination with the invasion of species that ultimately drives the turnover of communities (Fig. 2c, d). The intense replacement of species in these areas, located mainly within the Central Indo Pacific, may facilitate the formation of no-analogue assemblages, resulting in novel species associations and interactions[22]. Extensive areas experiencing little (31% and 77% of marine cells with total dissimilarity < 0.1 for the RCP8.5 and RCP4.5, respectively) or no (3% and 20% with 0 dissimilarity) change in community composition by 2100 also occur (Fig. 2a, b). These areas of low climate-change velocity, with strong temperature gradients or with stable future climatic conditions (Fig. S2), have good potential for protected areas resilient to climate change[3]. In the absence of extirpations, widespread invasions are projected to result in the strong biotic homogenization and increase in diversity of communities (Fig. 3), with different locations within regions sharing an increased number of species (Figs 1-2). Otherwise, regional spatial heterogeneity will increase for those areas where large numbers of species are extirpated (e.g., tropics under the RCP8.5), and for no-change areas (e.g., coastal areas of the Arctic under both scenarios). Though the outcome of invasions on biodiversity will depend on the nature of the interaction between invasive and resident species[23], our results highlight regions where such interactions are likely to be stronger under future climate change and could, consequently, be considered for inclusion in adaptive management monitoring programmes.

Comparison of projected (2006-2100) changes in species richness and community composition with contemporary (1985-2005) cumulative human impact[7] averaged across individual exclusive economic zones (EEZs) and sovereign regions highlights potential areas of conservation relevance for marine governance (Fig. 4 and Table S3). Overlap between high current human impact and large future changes in biodiversity (richness/composition) occurs under both RCPs within the EEZs of the Mediterranean, as well as across multiple tropical and subtropical regions such as the Caribbean (Antigua and Barbuda, Anguilla), India, the Bay of Bengal (Mynamar and Bangladesh), northern areas of the central Indo-Pacific

(Northern Mariana, Guam), and across the South and East China Sea. These areas should be considered for mitigation and restoration actions directed at reducing existing levels of other anthropogenic impacts, building resilience to effects of climate change. The fact that several of these EEZ ‘hotspots’ include some of the world’s most vexing maritime territorial disputes (e.g., Senkaku and Spartly islands, located respectively in the East and South China Seas) highlights the complex role that climate change might have for international ocean governance. The likely arrival of large numbers of climate migrants, and resulting compositional changes of present-day communities, could exacerbate tensions and strain negotiations over sovereignty with uncertain global repercussions[24]. At the other extreme, several EEZs currently experiencing low anthropogenic impact, including northern hemisphere high-latitude EEZs (Russia, Greenland, Alaska), Madagascar and south east Africa, Gulf of Guinea, and Australia, are projected to experience relatively large changes in community composition, despite prevailing low rates of species invasions under both RCPs (Fig. 4). These are areas where proactive conservation efforts directed towards preserving and protecting the integrity and functioning of current ecosystems, rather than maintenance of individual species, could be considered appropriate. Amongst these regions, the Coral Triangle and neighbouring EEZs emerge as unique in that the strongest contrasts between results associated with the two RCPs can be expected.

With current emissions tracking slightly above RCP8.5, preventing an increase in global temperature >2°C seems increasingly unlikely[13]. Both empirical[20] and modelled[5] evidence suggests that impacts of global warming on marine biodiversity are likely to be dramatically different within a very narrow margin of temperature increase. While our results support this hypothesis, they also suggest an intense redistribution of current biodiversity patterns regardless of the scenario followed. Centres of global marine biodiversity have shifted in location over geological timescales, mainly driven by major tectonic events[25], with current biodiversity patterns being established well before the Pleistocene over 2.5 million years ago. Our projections, however, suggest strongly that generalised changes in the global distribution of marine species will occur over the course of the century driven by anthropogenic climate change. These results de-emphasise biodiversity loss attributed directly to anthropogenic ocean warming but highlight the future global biotic homogenization of marine communities with stress due to novel biotic interactions. Current conservation plans will therefore need to anticipate and accommodate such changes, unprecedented in human history. Our results also reinforce current concerns over global warming and ocean governance[26] and their potential effects on the spatial mismatch between scales of governance and ecosystem conservation. Because effects of climate change will transcend jurisdictional borders, proactive conservation efforts should be made at adequate scales of governance through effective marine spatial planning, including, for example, promoting regional conservation frameworks for cross-country cooperation.

Methods. Climate data and velocity of climate change. We used projected (2006–2100) mean annual sea surface temperature (SST) data from multi-model ensemble means (Table S2) downloaded from the Royal Netherlands Meteorological Institute Climate Explorer portal (http://climexp.knmi.nl/about.cgi?id=rtisdale@snet.net). We distinguished three climate-change intervals within each scenario (see Supplemental Methods): early (2006-2040), mid (2041-2065) and late (2066-2100) 21st century (Fig. S1). Global 1°-resolution climate velocity (°C km^{-1}) maps[14] were produced for each combination of climate-change period and climate scenario (Fig. S2).

Species distribution maps. Modelled species distribution data (Table S1) were extracted from AquaMaps[18] using a minimum threshold likelihood of presence of 0.4 to convert from probability to binary (presence/absence) range maps. See the Supplemental Methods for a discussion on the choice of threshold and its effect on the resulting range maps used in our analysis.

Environmental temperature extremes and taxon-specific thermal tolerance limits. Environmental temperature extremes were defined from the multi-model ensemble mean SST data as the absolute maximum and minimum mean monthly SST projected for each simulation period and climate scenario. Species' thermal tolerance limits were estimated from baseline (1979-2009) climatology data as one standard deviation above/below the inter-annual mean of the annual maximum/minimum mean monthly SST within the species current range (Fig. S3).

Climate-niche trajectories and redistribution of species. Species' thermal-niche trajectories were projected by forward iteration of each 1° SST cell centroid within a species' distribution range at 10 time steps per year throughout the corresponding climate change period[3]. Displacement at each time step was determined from the speed and direction of local grid-cell climate velocity, giving latitudinal and longitudinal shifts. These were additionally constrained to a maximum of 1° longitude or latitude per time step. Obstructions by land barriers encountered in the path of a trajectory were solved by redirecting the trajectory towards the immediate non-diagonal neighbour cell having the coolest (warmest) SST given a positive (negative) local cell velocity. In the absence of a suitable neighbour cell (i.e., the focal cell having the local SST minimum or maximum) the trajectory was halted and that cell taken as the final niche location (see below).

The final distribution was estimated as those cells defining the location of the thermal niche at the start and end of the projection, together with the transition cells used to move from one to the other accounting explicitly for climate connectivity, filtered to satisfy the species' thermal tolerance and habitat requirements (see Supplemental Methods; Fig. S4). Thermal tolerance was checked by comparing the cell-based environmental temperature extremes for the projection period with the thermal tolerance range of the taxon. Because climate velocities and thermal niches are based on mean annual SST while thermal suitability is estimated from absolute mean monthly maximum and minimum SST, it is possible for part of the new thermal niche to be unsuitable due to the maximum/minimum temperature extremes being above/below the thermal tolerance for the species.

Habitat suitability was set in terms of depth and coastal affinity. Taxa were first classified as neritic or oceanic depending on whether ≥ 75% of their initial distribution was contained within coastal and shelf waters as defined by the marine ecoregions of the world (MEOW) classification[27]. MEOW boundaries are mainly set by depth (200-m isobath) restricted to a minimum of 370 km offshore. Neritic species were further classified as littoral species if ≥ 90% of their range fell within maritime coastline cells. The remaining species were classified as predominantly oceanic species with no particular habitat restriction. Movement of oceanic species was unrestricted in our model, while we imposed a restriction in depth (i.e. coastal and shelf waters) to neritic species.

Partitioning of temporal beta diversity. To estimate the contribution of temporal turnover (species replacement via co-occurring loss and gain) and nestedness (isolated species loss/gain leading to one community being a subset of the other) towards resulting cell-based changes in community composition between the start (2006) and end (2100) of our projections, we applied the additive partitioning of total β-diversity proposed by Baselga[28] for pairwise comparisons:

$$\beta_{\text{sor}} = \beta_{\text{sim}} + \beta_{\text{sne}} = \frac{b+c}{2a+b+c} = \frac{2b}{2b+a} + \left(\frac{c-b}{a+b+c}\right)\left(\frac{a}{2b+a}\right),$$

where β_{sor} refers to the total β-diversity calculated as Sørensen dissimilarity between the communities of a single cell at the start and end of the projection, accounting for both true turnover and nestedness, β_{sim} is the Simpson dissimilarity influenced only by turnover, and β_{sne} is the remaining nestedness component of β_{sor}. Between the two assemblages, *a* is the number of shared species while *b* and *c* refer to the number of unique species in the poorest and richest community between the two time points. Both components are bound by the value of total beta diversity (cannot be higher), and vary in a similar way between 0 (no nestedness/turnover) and 1.

Acknowledgments

This work was supported by the U.K. National Environmental Research Council grant NE/J024082/1. We acknowledge the World Climate Research Programme's Working Group on Coupled Modelling, responsible for CMIP, and thank the groups (Table S1) for producing and making available their model output.

Author contributions

All authors contributed to the conception and design of the study. B.S.H. provided species distribution data. J.G.M. and M.T.B. developed the model. J.G.M. conducted the analysis. All authors wrote the manuscript.

References

1. Hannah L, Ikegami M, Hole DG, Seo C, Butchart SHM, Peterson AT*, et al.* Global climate change adaptation priorities for biodiversity and food security. *PLoS ONE* 2013, **8**(8)**:** e72590.

2. Dornelas M, Gotelli NJ, McGill B, Shimadzu H, Moyes F, Sievers C*, et al.* Assemblage time series reveal biodiversity change but not systematic loss. *Science* 2014, **344**(6181)**:** 296-299.

3. Burrows MT, Schoeman DS, Richardson AJ, Molinos JG, Hoffmann A, Buckley LB*, et al.* Geographical limits to species-range shifts are suggested by climate velocity. *Nature* 2014, **507**(7493)**:** 492-495.

4. Moss RH, Edmonds JA, Hibbard KA, Manning MR, Rose SK, van Vuuren DP*, et al.* The next generation of scenarios for climate change research and assessment. *Nature* 2010, **463**(7282)**:** 747-756.

5. Cheung WWL, Lam VWY, Sarmiento JL, Kearney K, Watson R, Pauly D. Projecting global marine biodiversity impacts under climate change scenarios. *Fish and Fisheries* 2009, **10**(3)**:** 235-251.

6. Jones MC, Cheung WWL. Multi-model ensemble projections of climate change effects on global marine biodiversity. *ICES Journal of Marine Science: Journal du Conseil* 2014.

7. Halpern BS, Walbridge S, Selkoe KA, Kappel CV, Micheli F, D'Agrosa C*, et al.* A global map of human impact on marine ecosystems. *Science* 2008, **319**(5865)**:** 948-952.

8. Leadley P, Pereira HM, Alkemade R, Fernandez-Manjarrés JF, Proença V, Scharlemann JPW*, et al.* Biodiversity scenarios: Projections of 21st century change in biodiversity and associated ecosystem services. Montreal, Canada: Secretariat of the Convention on Biological Diversity; 2010. Report No.: 92-9225-219-4.

9. Munday PL, Warner RR, Monro K, Pandolfi JM, Marshall DJ. Predicting evolutionary responses to climate change in the sea. *Ecology Letters* 2013, **16**(12)**:** 1488-1500.

10. Poloczanska ES, Brown CJ, Sydeman WJ, Kiessling W, Schoeman DS, Moore PJ*, et al.* Global imprint of climate change on marine life. *Nature Clim Change* 2013, **3**(10)**:** 919-925.

11. Pinsky ML, Worm B, Fogarty MJ, Sarmiento JL, Levin SA. Marine taxa track local climate velocities. *Science* 2013, **341**(6151)**:** 1239-1242.

12. Chen I-C, Hill JK, Ohlemüller R, Roy DB, Thomas CD. Rapid range shifts of species associated with high levels of climate warming. *Science* 2011, **333**(6045)**:** 1024-1026.

13. Peters GP, Andrew RM, Boden T, Canadell JG, Ciais P, Le Quere C*, et al.* The challenge to keep global warming below 2 ˚C. *Nature Clim Change* 2013, **3**(1)**:** 4-6.

14. Loarie SR, Duffy PB, Hamilton H, Asner GP, Field CB, Ackerly DD. The velocity of climate change. *Nature* 2009, **462**(7276)**:** 1052-1055.

15. Hiddink JG, Burrows MT, García Molinos J. Temperature tracking by North Sea benthic invertebrates in response to climate change. *Global Change Biology* 2014**:** n/a-n/a.

16. Pereira HM, Leadley PW, Proença V, Alkemade R, Scharlemann JPW, Fernandez-Manjarrés JF*, et al.* Scenarios for global biodiversity in the 21st century. *Science* 2010, **330**(6010)**:** 1496-1501.

17. Van Dyke F. *Conservation Biology. Foundations, Concepts, Applications*, 2nd edn. Springer Science: Dordrecht, 2008.

18. Kaschner K, Rius-Barile J, Kesner-Reyes K, Garilao C, Kullander SO, Rees T*, et al.* AquaMaps: Predicted range maps for aquatic species. World wide web electronic publication. *wwwaquamapsorg Version 08/2013* 2013.

19. Kiessling W, Simpson C, Beck B, Mewis H, Pandolfi JM. Equatorial decline of reef corals during the last Pleistocene interglacial. *Proceedings of the National Academy of Sciences, USA* 2012, **109**(52)**:** 21378-21383.

20. Nguyen KDT, Morley SA, Lai C-H, Clark MS, Tan KS, Bates AE*, et al.* Upper temperature limits of tropical marine ectotherms: global warming implications. *PLoS ONE* 2011, **6**(12)**:** e29340.

21. Somero GN. The physiology of climate change: how potentials for acclimatization and genetic adaptation will determine 'winners' and 'losers'. *The Journal of Experimental Biology* 2010, **213**(6)**:** 912-920.

22. Blois JL, Zarnetske PL, Fitzpatrick MC, Finnegan S. Climate change and the past, present, and future of biotic interactions. *Science* 2013, **341**(6145)**:** 499-504.

23. Araújo MB, Luoto M. The importance of biotic interactions for modelling species distributions under climate change. *Global Ecology and Biogeography* 2007, **16**(6)**:** 743-753.

24. Koo MG. *Island Disputes and Maritime Regime Building in East Asia*. Springer Verlag: New York, 2009.

25. Renema W, Bellwood DR, Braga JC, Bromfield K, Hall R, Johnson KG*, et al.* Hopping hotspots: global shifts in marine biodiversity. *Science* 2008, **321**(5889)**:** 654-657.

26. Craig RK. Ocean governance for the 21st century: making marine zoning climate change adaptable. *Harvard Environmental Law Review* 2012, **36**(2)**:** 305-350.

27. Spalding MD, Fox HE, Allen GR, Davidson N, Ferdaña ZA, Finlayson MAX*, et al.* Marine ecoregions of the World: a bioregionalization of coastal and shelf areas. *BioScience* 2007, **57**(7)**:** 573-583.

28. Baselga A. Partitioning the turnover and nestedness components of beta diversity. *Global Ecology and Biogeography* 2010, **19**(1)**:** 134-143.

Figures

Figure 1. Redistribution of global biodiversity patterns under future climate change. (**a**) Total current species richness (*n* = 12,796). (**b, c**) Differences between current (year 2006) and projected (year 2100) (**b**) RCP4.5 and (**c**) RCP8.5 cell species richness. Black contour lines correspond to limits of Exclusive Economic Zones (EEZ). Latitudinal and longitudinal global medians with their 25 and 75% quartiles (5° moving average) are given in the marginal panels.

Figure 2. Partitioning of cell-based temporal β-diversity under future climate change. (**a, b**) Patterns in total β-diversity expressed as cell-based Sørensen dissimilarities (0 = no dissimilarity) between present-day (2006) communities and those projected for 2100, and its corresponding additive decomposition[28] (i.e., a = c + e; b = d + f) into (**c, d**) true temporal turnover (i.e. species replacement) and (**e, f**) nestedness (i.e., isolated local extinctions or invasions) for (**a, c, e**) RCP4.5 and (**b, d, f**) RCP8.5. Black contour lines correspond to EEZ limits.

Figure 3. Spatial homogenization of present-day communities under future climate change. (**a, b**) Projected 2006-2100 spatial variation in Sørensen dissimilarities between cell-based communities and the regional species pool, comprising all species present within the corresponding MEOW realm[27] and the High Seas, between 2006 and 2100 for (**a**) RCP4.5 and (**b**) RCP8.5. Negative values denote a decrease in dissimilarity (i.e., increased spatial homogenization). Black lines represent MEOW realm limits as identified in the lower panel (white area corresponding to the High Seas region).

Figure 4. Projected changes in species richness and community composition in relation to contemporary human impacts. (**a, d**) Choropleth maps showing relationships between contemporary (1985-2005) mean cumulative human impact index[7] and (**a, b**) projected (2006-2100) mean differences in total richness and (**c, d**) mean composition dissimilarities (total temporal β-diversity) within EEZ regions for (**a, c**) RCP4.5 and (**b, d**) RCP8.5. Colour category breaks correspond to the 25 and 75 quartiles for each variable, with exception of total richness for the RCP8.5, which also includes the 5% quantile to highlight EEZs with a high net decrease in richness. Refer to Table S3 for a detailed account by EEZ.

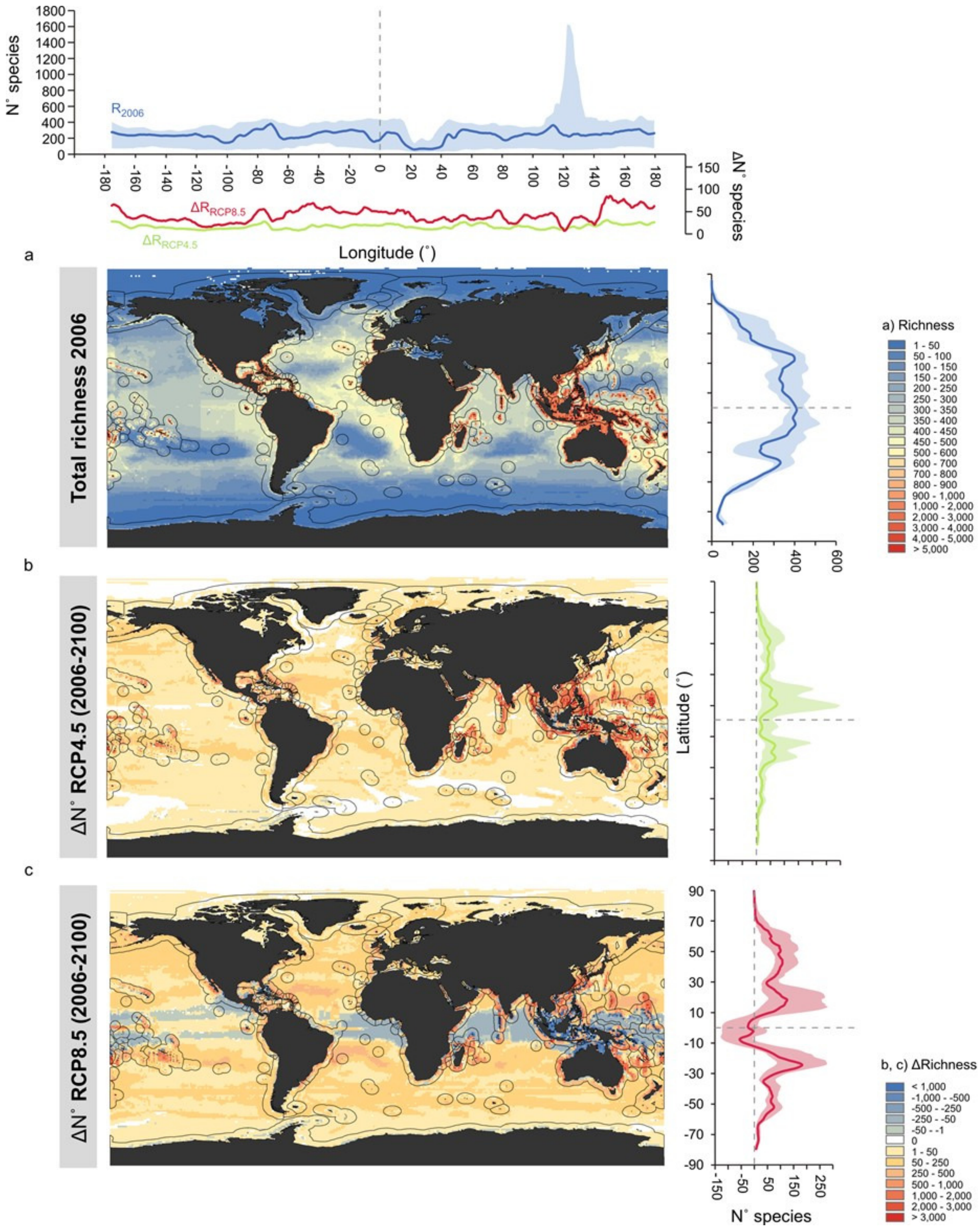

Figure 1. García Molinos et al.

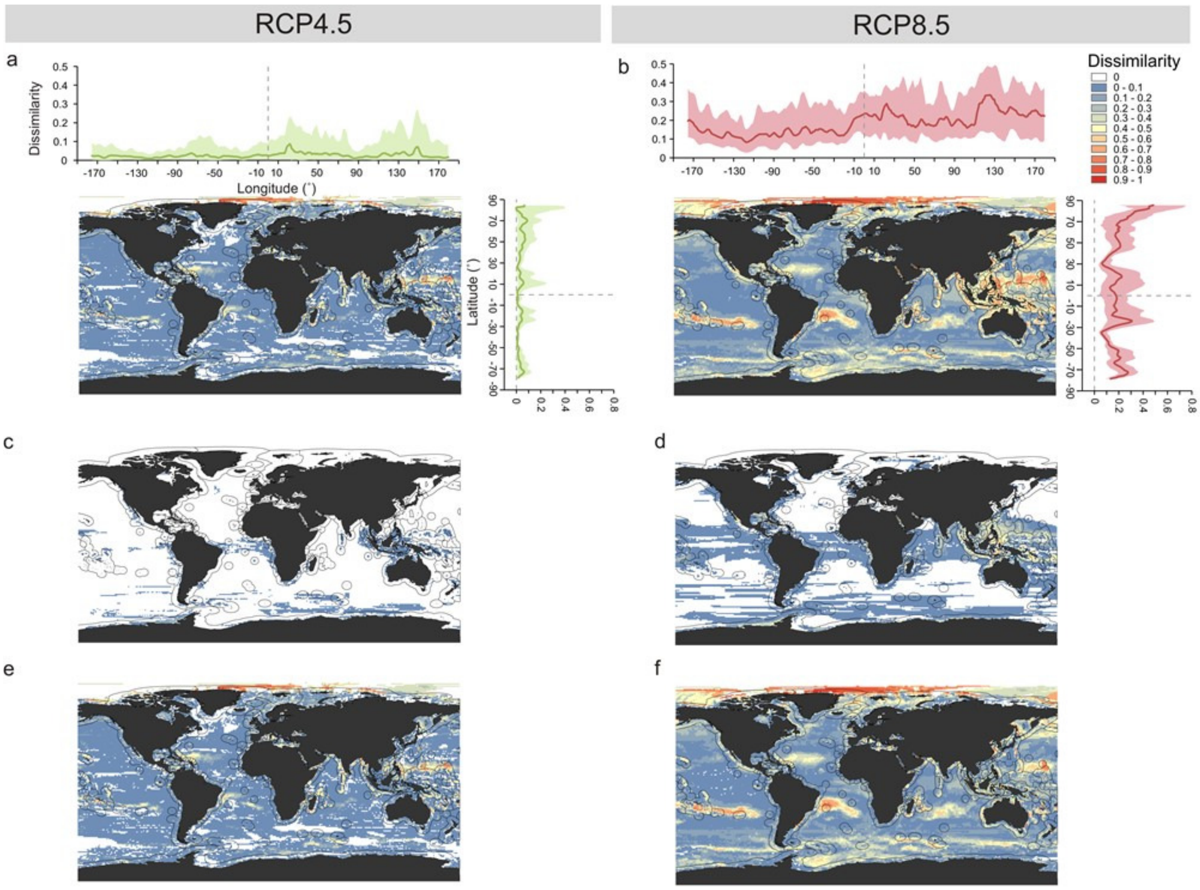

Figure 2. García Molinos et al.

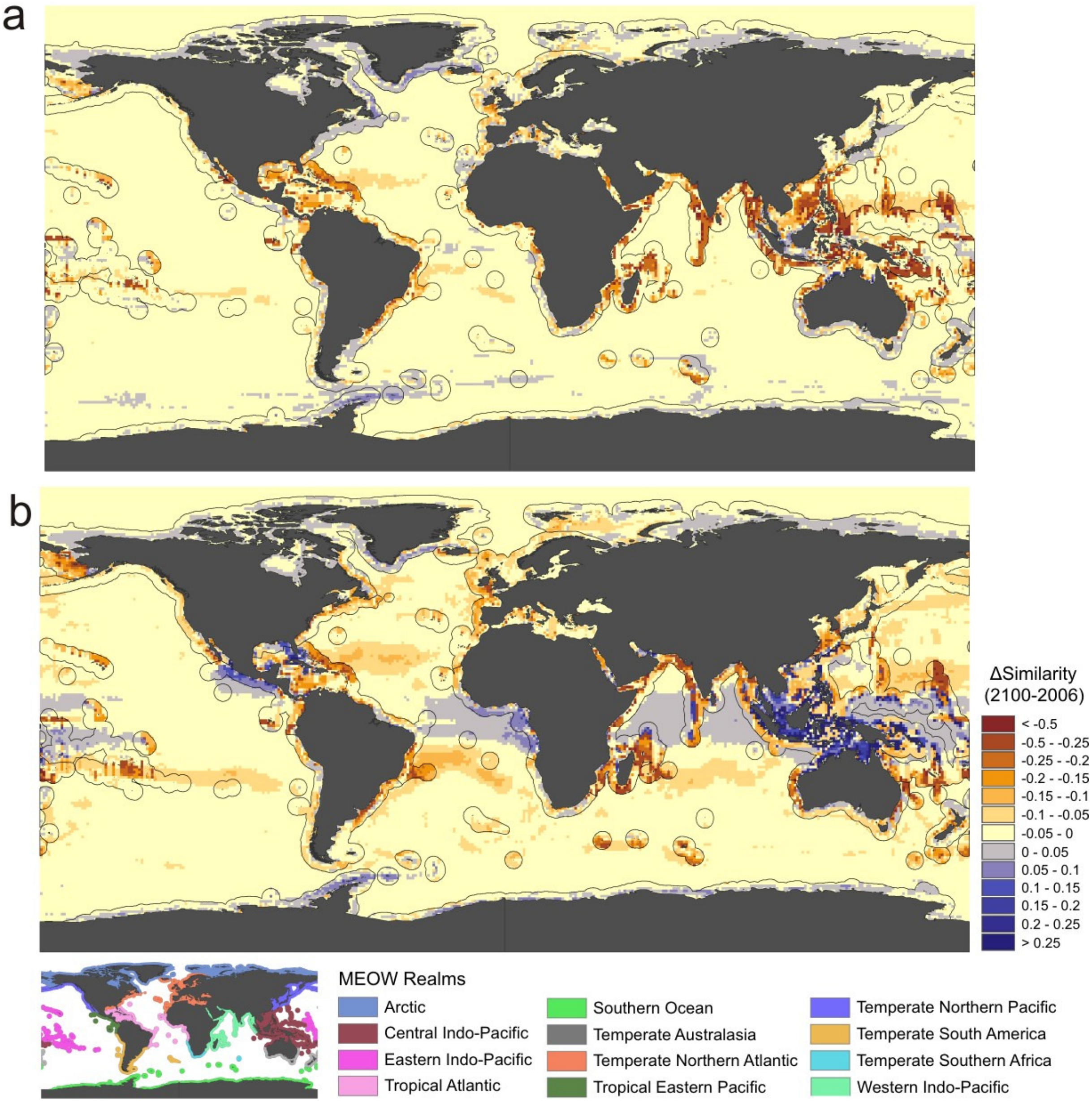

Figure 3. García Molinos et al.

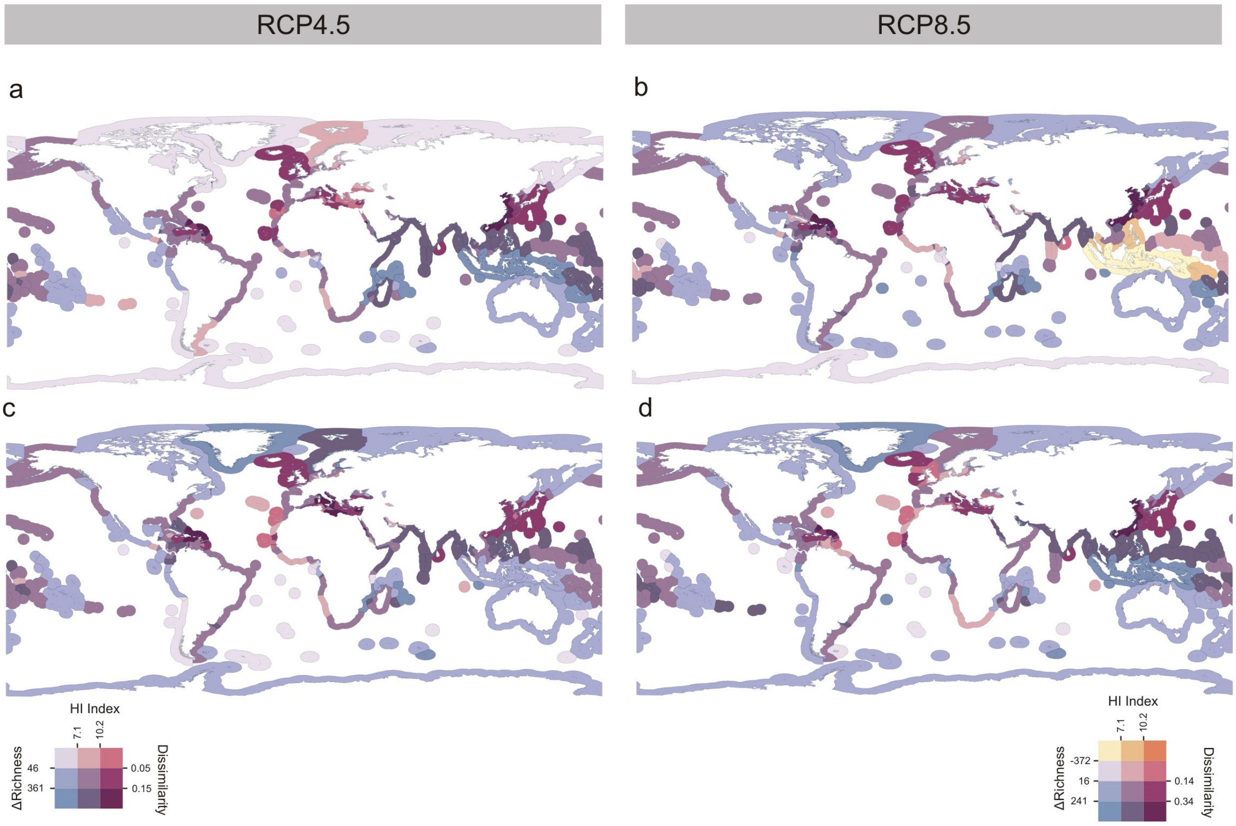

Figure 4. García Molinos et al.

Supplementary Information for

Climate velocity and the future global redistribution of marine biodiversity

Jorge García Molinos, Benjamin S. Halpern, David S. Schoeman, Christopher J. Brown, Wolfgang Kiessling, Pippa J. Moore, John M. Pandolfi, Elvira S. Poloczanska, Anthony J. Richardson, and Michael T. Burrows

Supplementary Methods

Climate Data and velocity of climate change

We used projected (2006–2100) mean annual sea surface temperature (SST) data from multi-model ensemble means (Table S2) for two IPCC RCPs representing a 'emissions stabilization' (RCP 4.5) and a 'business as usual' (RCP 8.5) climate scenario[4]. RCP8.5 represents a rising pathway scenario characterized by an increasing greenhouse gas emission trajectory over time (Fig. S1), working on the assumption of a >8.5 W m^2 radiative forcing by 2100 relative to pre-industrial values. The RCP4.5 represents a scenario where total radiative forcing is stabilized at ~4.5 W m^2 shortly after 2100 and in which temperatures rise at a rate comparable to that of the RCP8.5 during the first decades of the century, but slow progressively thereafter. RCP8.5 yields the highest rates of warming, with global mean sea-surface temperature in 2100 increasing by 2.4 ˚C relative to 2006 levels (corresponding ocean warming of 1 ˚C is expected for RCP4.5). Ensemble means were extracted from the Royal Netherlands Meteorological Institute Climate Explorer portal (http://climexp.knmi.nl/about.cgi?id=rtisdale@snet.net) based on individual model outputs sourced from the Coupled Model Intercomparison Project phase 5 (CMIP5).

To account for the differences in the rate of change in temperature, and hence climate velocity, over time we distinguished three climate-change projection periods within each climate-change scenario: early (2006-2040), mid (2041-2065) and late (2066-2100) 21st century. Thresholds between periods were set to accommodate detected statistically significant ($\alpha = 0.05$) changes in SST linear trend in both climate scenarios using the generic change-detection algorithm for time series BFAST (Breaks For Additive Seasonal and Trend)[31] (Fig. S1). Global 1º-resolution climate velocity (°C km^{-1}) maps (Fig. S2) were produced for each combination of climate change period and climate scenario by dividing the corresponding SST linear trend (°C yr^{-1}) by the spatial gradient (°C km^{-1}) using the associated spatial angles as an estimate of direction[14].

Species distribution maps

Modelled species distribution data (Table S1) were extracted from AquaMaps[18]. AquaMaps maps predict relative probabilities of species occurrence (0-1 range) derived from an environmental niche envelope model supplemented with species-specific information from occurrence records and, where available, expert knowledge (6.6% of the maps available as for 08.12.2014). Transfer of these probabilities into presence/absence range maps implicitly ignores niche suitability information, which can overestimate the range of cosmopolitan species in marginally suitable areas (e.g., truly oceanic species on shelf areas). This effect is customarily controlled by imposing a probability threshold on species presence that restricts the resulting range map to those regions of high environmental suitability for the species (i.e., core range). The influence of the choice of threshold on the resulting range maps is species-specific and mainly dependent upon the environmental specificity of the species defining the probability of occurrence distribution. Importantly to the type of analysis conducted here, previous studies using data sets sourced from AquaMaps have demonstrated that resulting global biodiversity patterns are largely insensitive to this parameter for moderate thresholds (< 0.5)[5, 30]. In general, ranges of widespread generalists, associated to multiple environments with different probability of occurrence, are the most affected while endemic or habitat specialists are relatively insensitive because they have a high probability of occurrence across their entire range. Here we used an arbitrary minimum threshold of 0.4, resulting in an overall range reduction of -24 ± 14 % (mean ± 1 SD) from that generated by using a non-exclusive approach (species presence defined by probability of occurrence > 0), with considerable among-phyla variation (Table S1).

Resulting distribution maps (0.5˚-resolution) were subsequently up-scaled to match the 1˚-resolution of the climate data by applying a ≥ 50% cell occupancy criterion to assign cell presence (i.e., two or more of the four 0.5˚ cells occupied). This is a subjective, though logical, choice that exclusively affects cells at the range edges and depends on the actual shape of the distribution range (e.g., range variation higher for convoluted than regular shapes). Relative to ranges defined by the adopted 0.5 threshold, the use of a more conservative (4 cells out of 4) or inclusive (1 cell out of 4) criterion resulted in mean range variations across all taxa of -61 ± 20 % and 24 ± 9 %, respectively.

Environmental temperature extremes and taxon-specific thermal tolerance limits

Environmental temperature extremes for each projected period were defined from the multi-model ensemble mean SST data as the maximum and minimum mean monthly SST within that period for each climate scenario. Species' thermal tolerance limits were estimated from the 1º-resolution HadISST 1.1 global sea-ice and SST data baseline (1979-2009) climatology as one standard deviation above/below the inter-annual mean of the annual maximum/minimum mean monthly SST within the species' initial (2006) range (Fig. S3). Given the lack of experimental data for most of the species, our definition of the thermal tolerance limits is subjective but pragmatic. Specifically, it intends to incorporate the potential effect of historical variability in mean SST: the greater the magnitude of temperature variation within a species' range, the wider physiological windows are expected to be in poikilothermic animals (i.e., the climate variability hypothesis)[32]. Nevertheless, because this parameter is likely to have a strong influence on model projections (see next section for a description of the modelling process), we conducted sensitivity analysis to examine how the selection of more (i.e., ± 2 SD) or less (i.e., using only the mean) conservative thermal limits would influence model outputs (Fig. S6). Whereas patterns of leading-edge expansions (i.e., invasions) remained unaltered irrespective of the minimum thermal limit chosen (results not shown), selection of the maximum thermal limit influenced strongly the number of trailing-edge contractions (i.e., extirpations), particularly under RCP8.5, though their geographical patterns were in general good agreement (Fig. S7). Defining thermal tolerances for marine ectotherms based on their distribution ranges is a reasonable approach in the absence of empirical data because they are mainly thermal range conformers[33] (i.e., they tend to occupy fully their potential thermal niche). However, we still know very little about the actual contribution of natural variability towards their thermal tolerance limits. Irrespective, because empirical estimates of physiological thermal limits are themselves prone to bias resulting from plasticity to environmental constraints[34], no approach is likely to give the true answer.

<u>Climate niche trajectories and redistribution of species</u>

Given the realized thermal niche of a species i at time t (N_i^t), defined by its current distribution (D_i^t) and assumed to be equal to its potential thermal niche, its distribution at the end year of the simulation period (D_i^{t+n}) was calculated as follows (Fig. S4):

1. Estimate the new location of the **thermal niche** (N_i^{t+n}) by projecting each 1° cell contained within N_i^t in the direction and speed dictated by the corresponding cell velocities.
2. Define the new **potential distribution** for the species comprising the old (N_i^t) and new (N_i^{t+n}) thermal niches, together with all those intermediate cells used to reach N_i^{t+n} from N_i^t (Fig. S4a), thereby explicitly accounting for climate connectivity.
3. Estimate the final **realized distribution** of the species (D_i^{t+n}) by checking each cell within its potential distribution range against corresponding habitat and thermal filters:
    a. Presence cells were first checked for **habitat suitability** (Fig. S4b). Species were first classified by habitat as predominantly oceanic or neritic. Neritic

species (n = 11,462) found primarily over continental or island shelves were defined as species with ≥ 75% of their current distribution within limits of the marine ecoregions of the world (MEOW) proposed by Spalding et al.[27]. These ecoregions cover all coastal and shelf waters shallower than 200 m with a minimum offshore threshold of 370 km. We further divided neritic species into sublittoral (n = 3,100) and littoral (n = 8,362), defined as species having ≥ 90% of their range in maritime coastline cells, to capture species dependant on proximity to strictly littoral habitats. Cells from the initial distribution of neritic species falling outside habitat boundaries (1 ± 3.3 %; mean ± standard deviation) were therefore not projected, although they were kept as part of the final distribution if they met thermal criteria (see below). The remaining species were classified as oceanic species (n = 1,334) with no particular habitat restriction in terms of occupancy.

b. Comparison between the thermal tolerance limits of the species (defined from the max/min SST baseline climatology) and the cell-specific environmental temperature extremes gave thereafter an estimation of **thermal occupancy** with the following outcomes for local warming (Fig. S4d; thermal comparisons are reversed for a locally cooling area): (1) **range contraction** from areas currently occupied from which the species is extirpated as maximum temperature extremes exceed its upper thermal tolerance, (2) **distribution stasis** corresponding to areas where the species was originally found and that remain within the thermal tolerance limits for the species, (3) **range expansion** as areas currently not occupied and becoming thermally suitable for the species, and (4) **thermal intolerance** as new cells occupied by the thermal niche which the species can however not colonize because the minimum temperature extreme is below its lower thermal tolerance. Note that because climate velocities and thermal niches are based on mean annual SST while thermal suitability is estimated from absolute mean monthly maximum and minimum SST, it is possible for part of the new thermal niche to be unsuitable due to the maximum/minimum temperature extremes being above/below the thermal tolerance for the species.

4. The resulting new distribution (D_i^{t+n}) defines the new thermal niche for projection into the next climate change period.

Species thermal niche trajectories were projected as in Burrows et al.[3] by forward iteration of each 1º SST cell centroid within a species distribution range at 0.1-year time steps throughout the corresponding climate-change period. Displacement at each time step was determined from the speed and direction of local grid-cell climate velocity, giving latitudinal and longitudinal shifts after accounting for the distortion introduced by latitude on cell width (1˚ longitude = 111.325 * cos(ºlatitude) km) and limited to a maximum of 1º longitude or latitude per time step. Obstructions by land barriers encountered in the path of a trajectory were solved by redirecting the trajectory towards the immediate non-diagonal neighbour cell having the lowest (highest) SST, given a positive (negative) local cell velocity. A trajectory was halted in the absence of a suitable neighbour cell (i.e., the focal cell having the local SST minimum or maximum) and the cell taken as a potential final niche location.

Spatial homogenization in community composition

Spatial homogenization was calculated as cell-based Sørensen dissimilarity between local communities (i.e., individual 1º cells) and the corresponding regional species pool defined by all the species present within each single MEOW realm. Open-ocean cells falling outside realm borders were classified as High Seas and analysed separately. Differences between dissimilarities at the beginning (2006) and end (2100) of the projected period were used as an estimate of the expected extent of spatial homogenization experienced by present-day communities over the course of the century under both RCPs.

Supplementary Discussion

Our bioclimatic envelope model relies on a series of key assumptions that require further comment:

1. The central assumption of our model is that SST is the primary component of a species' climate niche, which it seeks to maintain over time. This is a widely supported notion[8, 9, 33]. We further assume that climate migrants will track their shifting thermal niches in the direction and at the rate dictated by local climate velocity. Supporting evidence on this assumption, though less established because of the relatively novelty of the climate velocity concept, is also strong[11, 15] and, importantly, robust to differences in life history[11]. Despite the general sensitivity of the distribution of marine species to global warming[11, 12], not all species will need to, or be able to, track their shifting thermal niches, and even when doing so they might show a lagged response[15], which will undoubtedly affect range dynamics.
2. By inferring changes in species distribution from shifts in thermal niche space, we have purposely omitted many other important biotic, abiotic and anthropogenic drivers. Ocean acidification is, for example, another global stressor expected to influence marine biodiversity strongly under future anthropogenic climate change. Because pH and the solubility of carbonate are naturally lower at higher latitudes due to the lower water temperatures, distribution shifts responding to ocean acidification (towards the equator) could be expected to counter those elicited by warming (polewards)[34]. However, unlike temperature, evidence linking changes in species distribution with on-going ocean acidification is lacking, and the long-term response of marine populations to ocean acidification remains uncertain. Because projections from species distribution models are highly sensitive to the choice of predictor variables[35], the trade-off between model complexity and applicability is dependent on

an adequate understanding of the factors driving that variation. Where this understanding is not available, simple models based on the fundamental relationships between key environmental variables and species distributions can arguably provide important insight into global biodiversity conservation.

3. Nevertheless, the velocity of climate change is ultimately a physical metric defining the speed and direction of change in isotherms over time and across space. Therefore, a distinction needs to be made between thermal shifts and the resulting redistribution of a species range. While we look at the movement of thermal niches as opportunities for a species to expand, areas from which the current thermal niche shifts away are left vacant by the species only if they become thermally unsuitable. In this way we reflect the fact that range contractions promoted by climate change are often slower than expansions of the leading edge[10] because they are driven primarily by extirpation of subpopulations as conditions surpass their tolerance limits.
4. Spatial predictions of distribution range from point occurrence data (e.g. Aquamaps maps) based on estimates of environmental preferences can be influenced by bias in sampling effort as well as by the selection of variables used to estimate the environmental envelopes, potentially leading to unrealistic distributions. Although it is obvious that predictions can be improved using better data (presence/absence) or increasing the sophistication of the models, this can only be done on a case-by-case basis and it is certainly unfeasible where the objective is to analyse multi-taxon range shifts and global biodiversity patterns in the ocean. Therefore, given the resources currently available, these limitations must be accepted and acknowledged. Aquamaps represent the most comprehensive data set of species distributions globally for marine species, frequently used for global projections of commercial fish and invertebrate species richness[5, 6]. Species' range maps modelled from environmental envelopes

based on presence-only species occurrence data, including AquaMaps, have been shown to perform reasonably well when compared to other existing niche modelling methods[6, 36].

5. Movement of neritic climate migrants in our model is restricted by depth as well as by geographical limits[3]. Although many of these coastal species have larval stages capable of dispersing long distances and traversing open waters, the extent to which their populations are demographically open is subject of current debate[37]. Ultimately, we consider larval dispersion to be primarily passive, driven by factors (e.g., currents) other than a direct response to climate change.
6. Although depth and coastal affinity might not reflect strict habitat requirements but simply covary with other biophysical factors, they are two parameters commonly used to parameterise species distribution models for global analys[6, 7]. This is because when there is little knowledge of the suite of environmental covariates for each individual species considered, projections made without depth and coastal affinity result in more uncertain and unrealistic projections.
7. The cumulative human impact index proposed by Halpern et al.[7] has a climate change element which includes SST (note, though, that these are anomalies not means), however their index refers to past (1985-2005) impacts, whereas our projections are based on climate-change velocity calculated from future SSTs (2006-2100). The lack of a temporal overlap between the temperature parameters therefore precludes a possible confounding effect. Further, the human impact index refer to local cumulative impacts and is thus spatially static (i.e., specific location or cell), whether our projections of biodiversity change are based on range shifts and emphasize therefore climate connectivity (i.e., movement of species in response to future climate

warming). We believe that crossing both effects is important for gaining better insight into future conservation and climate change adaptation needs.

Supplementary references

30. Selig ER, Turner WR, Troëng S, Wallace BP, Halpern BS, Kaschner K, et al. Global priorities for marine biodiversity conservation. PLoS ONE 2014, 9(1): e82898.

31. Verbesselt, J., Hyndman, R., Newnham, G. & Culvenor, D. Detecting trend and seasonal changes in satellite image time series. Remote Sens. Environ. **114**, 106-115 (2010).

32. Stevens, G. C. The latitudinal gradient in geographical range: how so many species coexist in the tropics. The American Naturalist **133**, 240-256 (1989).

33. Sunday, J. M., Bates, A. E. & Dulvy, N. K. Thermal tolerance and the global redistribution of animals. Nature Clim. Change **2**, 686-690 (2012).

34. van Hooidonk, R., Maynard, J. A., Manzello, D. & Planes, S. Opposite latitudinal gradients in projected ocean acidification and bleaching impacts on coral reefs. Global Change Biol. **20**, 103-112 (2014).

35. Synes, N. W. & Osborne, P. E. Choice of predictor variables as a source of uncertainty in continental-scale species distribution modelling under climate change. Global Ecol. Biogeogr. **20**, 904-914 (2011).

36. Ready, J. et al. Predicting the distributions of marine organisms at the global scale. Ecol. Model. **221**, 467-478 (2010).

37. Cowen, R. K. & Sponaugle, S. Larval dispersal and marine population connectivity. Annu. Rev. Mar. Sci. **1**, 443-466 (2009)

Supplementary Figures

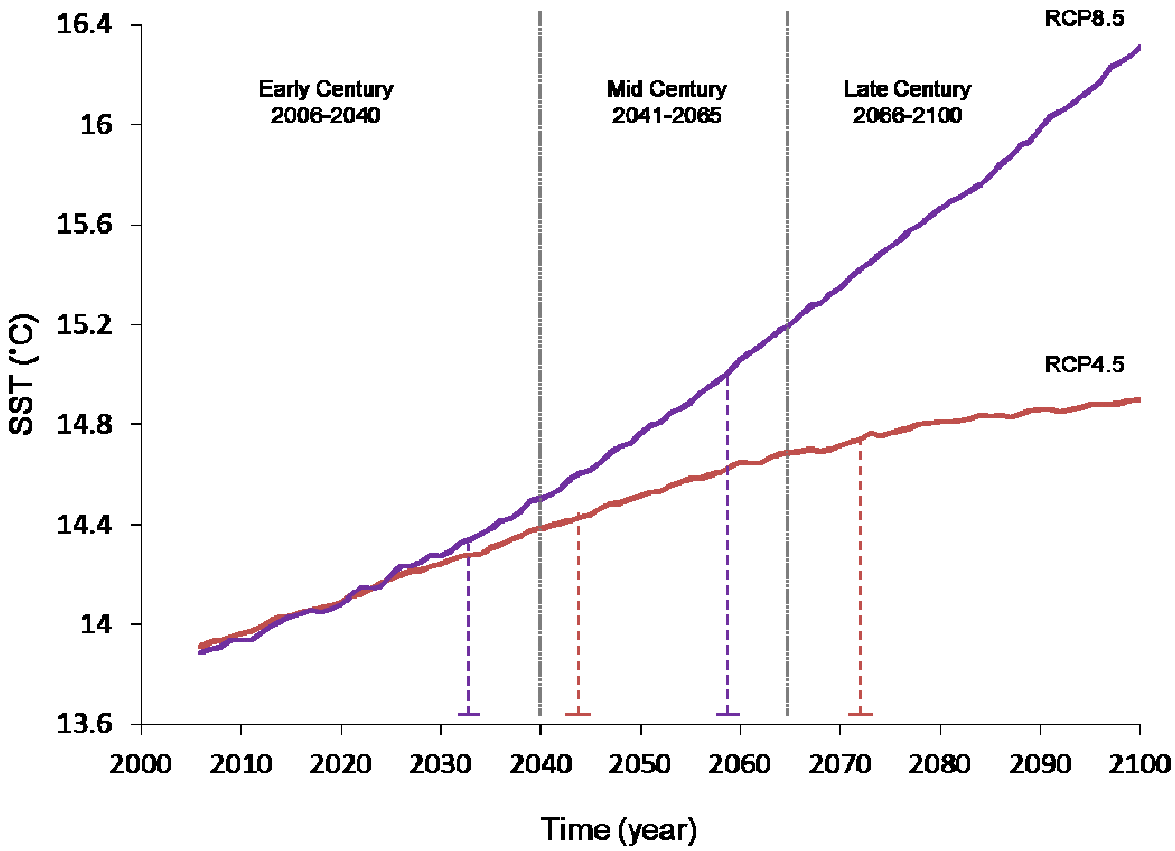

Figure S1. Global mean SST from multi-model ensemble mean RCP8.5 and RCP4.5 scenarios. Vertical dotted lines indicate the boundaries between climate change periods used for projection of species distributions set to accommodate detected significant changes in SST linear trend between climate scenarios (indicated by the dashed vertical lines with horizontal bars for their 95% CI).

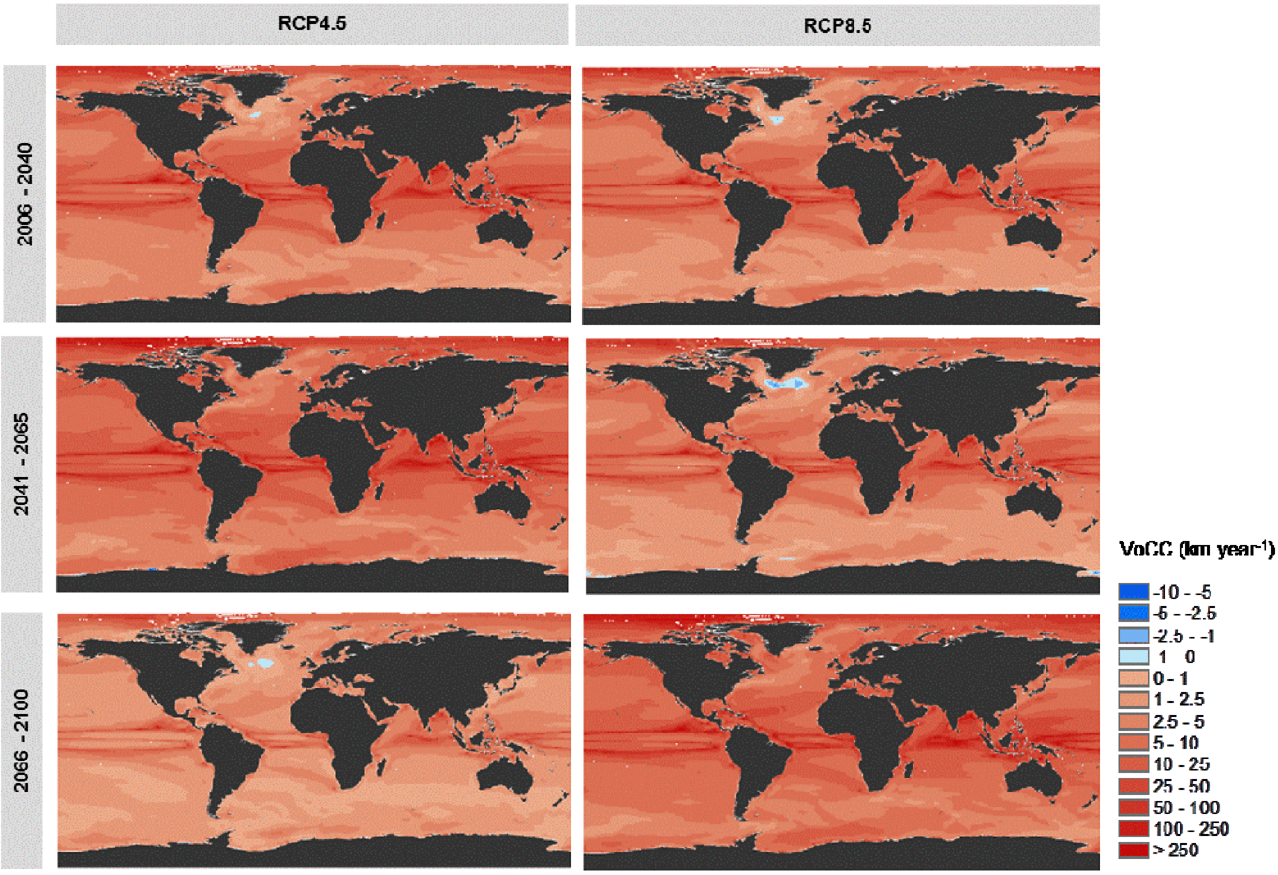

Figure S2. The velocity of climate change for each time period and scenario.

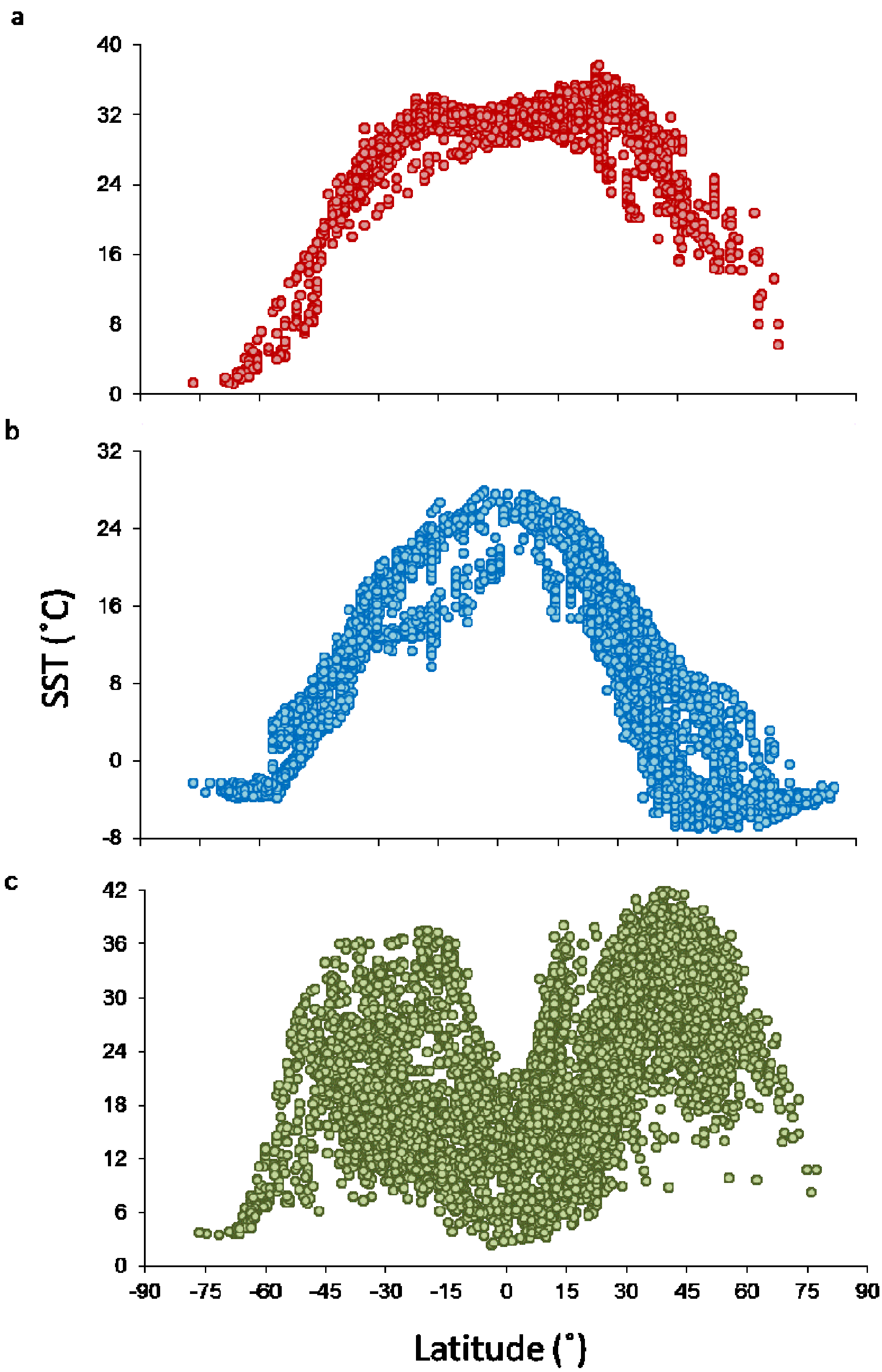

Figure S3. Latitudinal distribution of thermal tolerances. a) maximum and (**b**) minimum thermal tolerance limits within the current distribution range for the studied species (n = 12,796) used for the velocity trajectory projections estimated from a base-line (1979-2009) climatology of mean monthly SST (HadISST) as the maximum/minimum inter-annual cell mean sea surface temperature ± 1 standard deviation. **c**) Thermal tolerance range (latitudes given as the middle point between max and min latitudes).

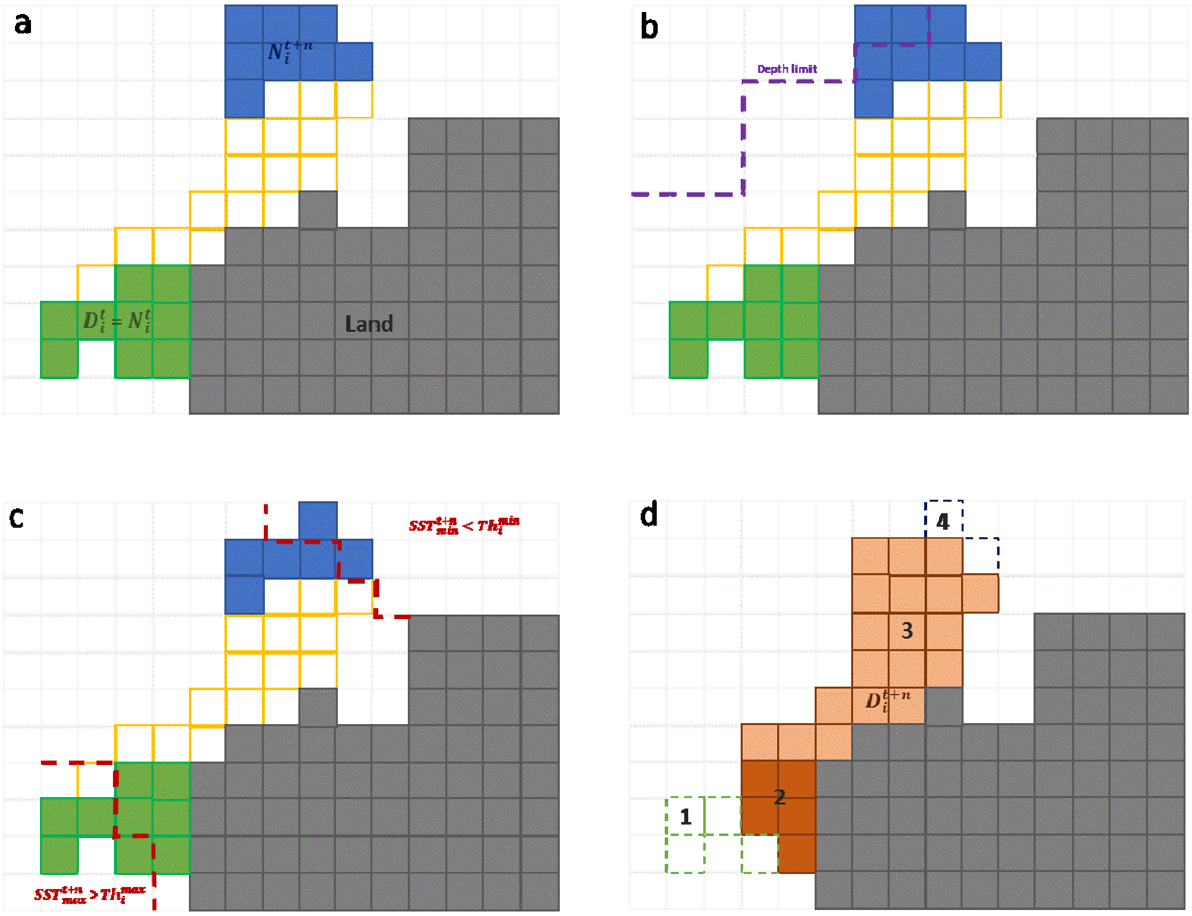

Figure S4. Schematic of the process followed to project the future distribution of a species based on the trajectories followed by its thermal envelope. Assuming a species *i* fully occupies its thermal niche at a given time *t* (i.e., its potential and realized thermal niches are the same $D_i^t = N_i^t$), its distribution at time *t+n* is estimated by (a) determining the new location for its thermal niche (blue cells) by projecting each cell within its current range (green cells) following the direction and speed dictated by the cell-specific climate velocities. The resulting new potential distribution for the species comprises the old and new location of its thermal niche together with all the intermediate cells (unfilled yellow cells) through which the niche passed to reach its final position. Presence or absence of the species at each cell within the new domain is thereafter determined by (b) checking for habitat suitability (i.e., removing cells falling outside depth limits for neritic sublittoral species) and (c) checking for thermal occupancy by comparing the corresponding cell temperature extremes ($SST^{t+n}_{max/min}$) with the species' thermal tolerance limits ($Th_i^{max/min}$) with four possible outcomes (d): (1) *range contraction* (green dashed cells) from areas currently occupied from which the species is extirpated as maximum temperature extremes exceed its upper thermal tolerance, (2) *distribution stasis* (dark brown cells) are areas where the species was originally found and that remain within the thermal tolerance limits for the species, (3) *range expansion* (light brown cells) as areas currently not occupied and becoming thermally suitable for the species, and (4) *thermal intolerance* (dashed blue cells) as new cells occupied by the thermal niche which the species can however not colonize because the minimum temperature extreme is below its lower thermal tolerance. The resulting realized distribution (D_i^{t+n} ; brown cells) is then used as the new thermal niche for projection into the next time point. Note that because climate velocities and thermal niches are based on mean annual SST while thermal suitability is estimated from absolute mean monthly maximum and minimum SST, it is possible for part of the new thermal niche to be unsuitable due to the maximum/minimum temperature extremes being above/below the thermal tolerance for the species.

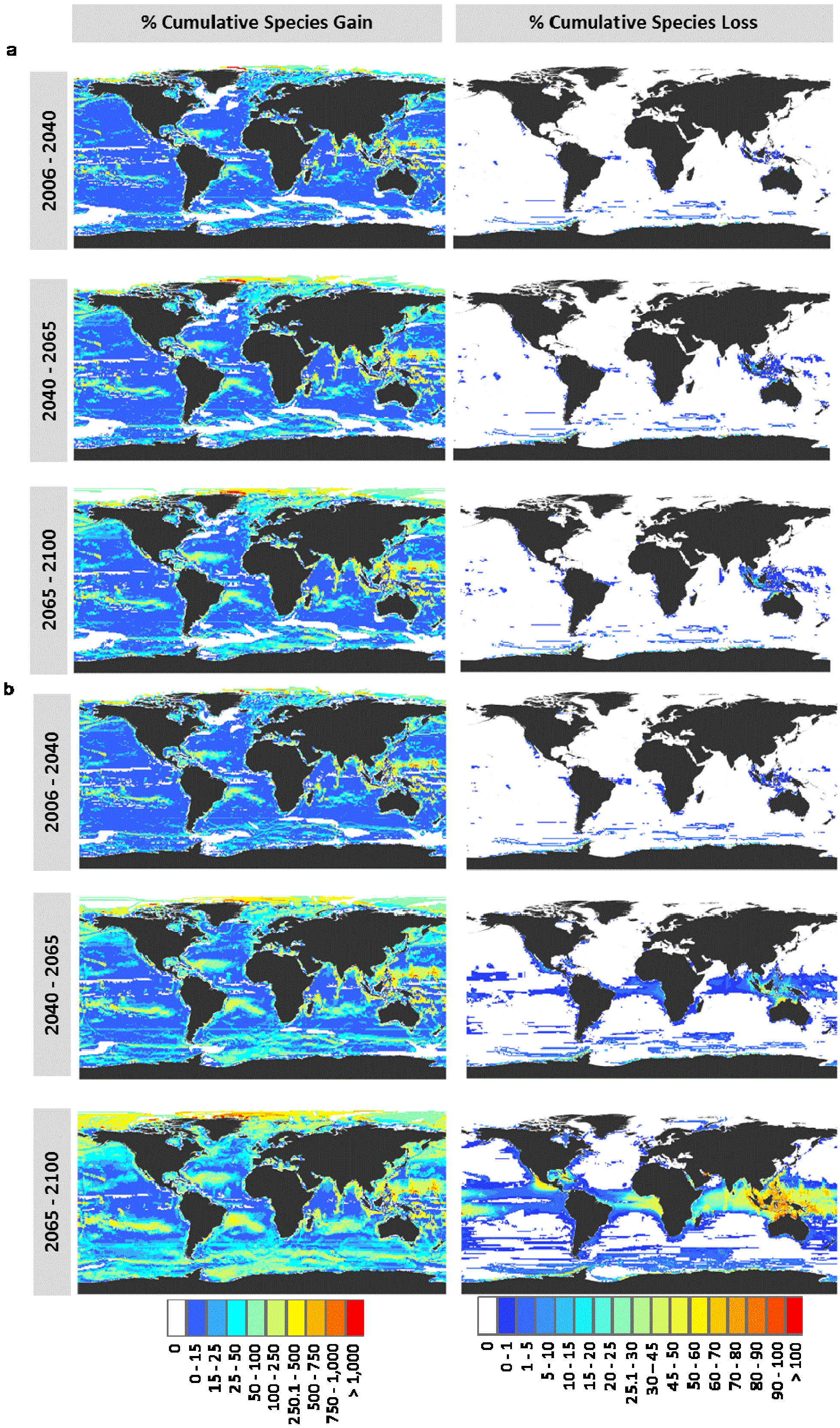

Figure S5. Cumulative percentage of species gained and lost at the end of each climate change period under (a) RCP8.5 and (b) RCP4.5 scenarios. Percentages of species gained and lost are calculated for each period by reference to the number of species per cell at the starting point of a period.

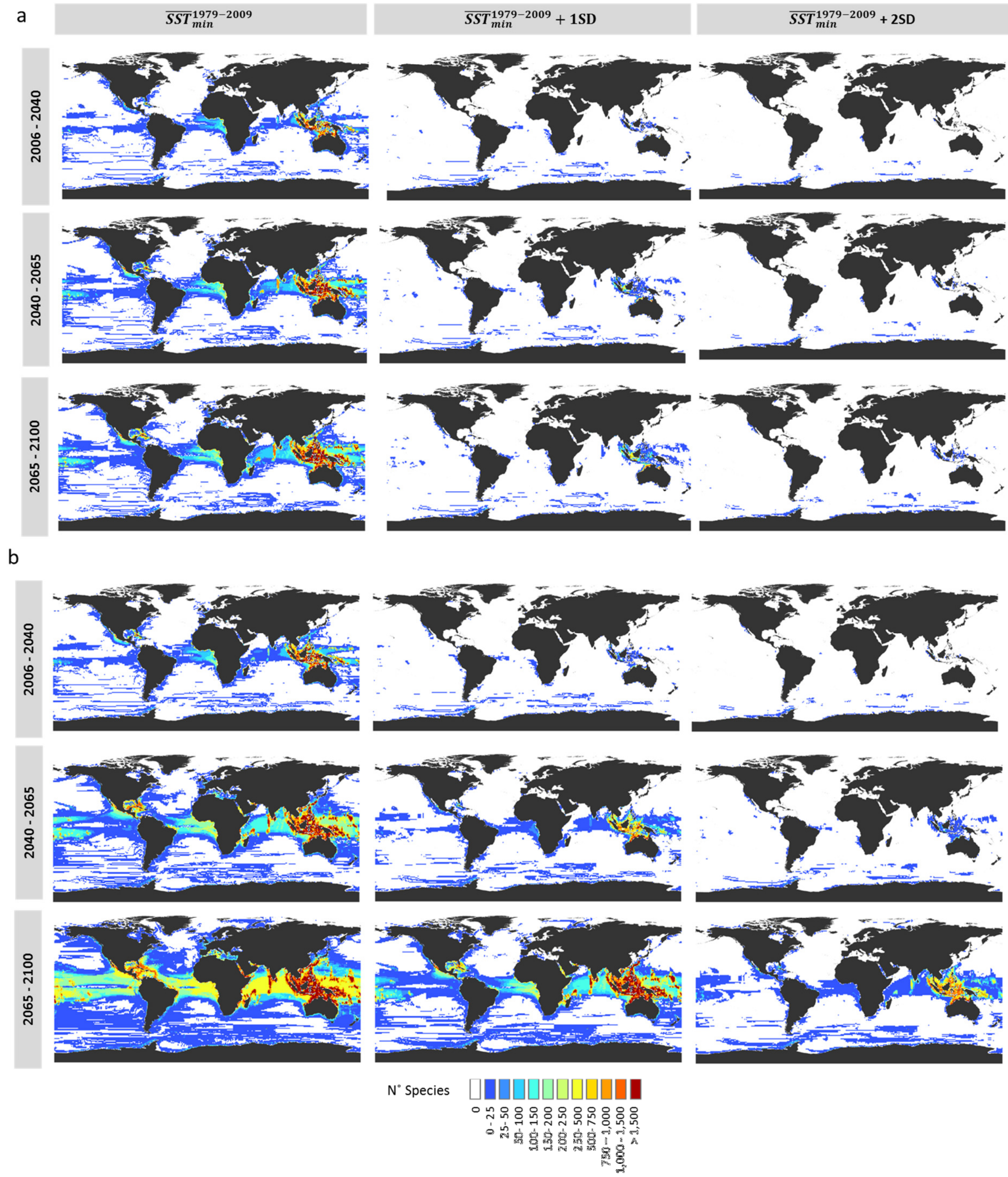

Figure S6. Sensitivity analysis on the taxonomic maximum thermal tolerance limit. Cumulative number of species lost over each projected climate change interval for (**a**) RCP4.5 and (**b**) RCP8.5 scenario resulting from using different estimates of the maximum thermal tolerance limit for the species: just the inter-annual mean of the historical annual maximum mean monthly SST within the species current range ($\overline{SST}_{min}^{1979-2009}$), or adding 1 or 2 standard deviations above the mean to account for environmental variability.

Supplementary Tables

Table S1. List of phyla included in the analysis with their corresponding number of species and the variation in range (proportion) produced by adopting a 0.4 probability of occurrence threshold as compared to a non-exclusive criterion (i.e., presence where probability > 0).

Phylum	Example of groups included	Number of Species	ΔRange Probability threshold
Acanthocephala	Thorny-headed worms	1	-0.5
Annelida	Ringed worms	35	-0.45 ± 0.15
Arthropoda	Crustaceans	687	-0.28 ± 0.16
Brachiopoda	Lamp shells	11	-0.34 ± 0.11
Bryozoa	Moss animals	24	-032 ± 0.14
Cephalorhyncha	Invertebrates	3	-0.21 ± 0.1
Chaetognatha	Arrow worms	14	-0.28 ± 0.11
Chlorophyta	Green algae	19	-0.17 ± 0.12
Chordata	Angle fishes, butterfly fishes, groupers, hagfishes, tunas and billfishes, sharks, skates and rays, mammals, reptiles, parrot fish, wrasses, others	9,475	-0.24 ± 0.17
Cnidaria	Corals, jellyfishes	906	-0.18 ± 0.11
Ctenophora	Comb jellies	2	-0.63 ± 0.16
Echinodermata	Starfishes, sea urchins, sand dollars, sea cucumbers	67	-0.22 ± 0.15
Entocprocta	Other (invertebrates)	1	-0.18
Gastrotricha	Hairybacks	12	-0.15 ± 0.1
Mollusca	Molluscs	1,298	-0.23 ± 0.14
Nemertea	Ribbon worms	1	-0.21
Ochrophyta	Other (invertebrates)	15	-0.16 ± 0.09
Phoronida	Horseshoe worms	1	-0.26
Polypodiophyta	Mangroves	3	-0.16 ± 0.08
Porifera	Sponges	30	-0.32 ± 0.18
Rhodophyta	Red algae	19	-0.16 ± 0.1
Sipuncula	Peanut worms	35	-0.42 ± 0.16
Tracheophyta	Sea grasses, mangroves	134	-0.17 ± 0.03
Not assigned	Others	3	-0.26 ± 0.11
TOTAL		**12,796**	**-0.24 ± 0.14**

Table S2. Model names and institutions that provided the model output on which the multi-model ensemble means used in this study are based (extracted from the Royal Netherlands Meteorological Institute Climate Explorer portal http://climexp.knmi.nl/about.cgi?id=rtisdale@snet.net).

Modeling Center (or Group)	Institute ID	Model Name
Commonwealth Scientific and Industrial Research Organization (CSIRO) and Bureau of Meteorology (BOM), Australia	CSIRO-BOM	ACCESS1.0 ACCESS1.3
Beijing Climate Center, China Meteorological Administration	BCC	BCC-CSM1.1 BCC-CSM1.1(m)
Canadian Centre for Climate Modelling and Analysis	CCCMA	CanESM2
University of Miami - RSMAS	RSMAS	CCSM4(RSMAS)*
Community Earth System Model Contributors	NSF-DOE-NCAR	CESM1(BGC) CESM1(CAM5)
Centro Euro-Mediterraneo per I Cambiamenti Climatici	CMCC	CMCC-CM CMCC-CMS
Centre National de Recherches Météorologiques / Centre Européen de Recherche et Formation Avancée en Calcul Scientifique	CNRM-CERFACS	CNRM-CM5
Centre National de Recherches Météorologiques / Centre Européen de Recherche et Formation Avancée en Calcul Scientifique Commonwealth Scientific and Industrial Research Organization in collaboration with Queensland Climate Change Centre of Excellence EC-EARTH consortium	CNRM-CERFACS CSIRO-QCCCE EC-EARTH	CSIRO-Mk3.6.0
Centre National de Recherches Météorologiques / Centre Européen de Recherche et Formation Avancée en Calcul Scientifique Commonwealth Scientific and Industrial Research Organization in collaboration with Queensland Climate Change Centre of Excellence EC-EARTH consortium LASG, Institute of Atmospheric Physics, Chinese Academy of Sciences and CESS,Tsinghua University	CNRM-CERFACS CSIRO-QCCCE EC-EARTH LASG-CESS	EC-EARTH
The First Institute of Oceanography, SOA, China	FIO	FIO-ESM
NOAA Geophysical Fluid Dynamics Laboratory	NOAA GFDL	GFDL-CM3 GFDL-ESM2G GFDL-ESM2M
NASA Goddard Institute for Space Studies	NASA GISS	GISS-E2-H GISS-E2-R

Table S3. Mean cumulative human impact index and projected net change in species richness (ΔR) and composition (Sørensen dissimilarities, D) within exclusive economic zone (EEZ; *n* = 225) and sovereign region (*n* = 156) by year 2100 under the RCP4.5 and RCP8.5. Mean present-day (2006) species richness (R06) is also given for comparison. Ranks indicate the position of each sovereign (EEZ) in increasing order of magnitude for each variable (note that the lower ΔR ranks for the RCP8.5 correspond to high negative values). Mean values calculated as cell-averages within each EEZ (sovereign means weighted by EEZ area).

Sovereign / EEZ	R06	Rank		Impact	Rank		ΔR4.5	Rank		ΔR8.5	Rank		D4.5	Rank		D8.5	Rank	
Algeria	352	41	(65)	10.90	134	(193)	49	39	(59)	46	63	(74)	0.094	71	(106)	0.095	17	(25)
Angola	573	77	(130)	7.76	47	(74)	191	87	(133)	-2	36	(40)	0.081	60	(92)	0.311	110	(156)
Antarctica	57	8	(9)	3.26	2	(3)	6	8	(9)	10	45	(51)	0.076	55	(84)	0.217	67	(97)
Antigua and Barbuda	478	57	(93)	11.15	140	(200)	513	131	(192)	506	143	(205)	0.364	155	(220)	0.366	124	(177)
Argentina	232	27	(43)	7.64	41	(68)	43	37	(53)	117	90	(121)	0.056	37	(62)	0.197	58	(86)
Australia	946	117		6.72	25		303	109		201	114		0.091	67		0.277	97	
Australia	1128		(195)	6.73		(49)	353		(166)	203		(160)	0.091		(103)	0.282		(139)
Christmas Island	547		(120)	6.66		(46)	630		(205)	332		(184)	0.209		(199)	0.404		(191)
Cocos Islands	379		(70)	8.42		(97)	50		(63)	53		(79)	0.036		(39)	0.128		(47)
Heard and McDonald Islands	148		(26)	7.01		(54)	81		(85)	127		(125)	0.210		(200)	0.348		(171)
Macquarie Island	118		(24)	4.83		(12)	11		(14)	82		(98)	0.022		(24)	0.259		(130)
Norfolk Island	597		(139)	6.62		(43)	78		(82)	436		(198)	0.027		(30)	0.219		(98)
Australia - Papua New Guinea	4141	156	(225)	1.13	1	(1)	29	23	(31)	-2753	1	(1)	0.000	3	(3)	0.498	148	(213)
Australia/Indonesia	1712	145	(212)	6.22	17	(34)	1111	151	(220)	-472	7	(7)	0.119	95	(140)	0.492	147	(211)
Bahamas	973	121	(185)	8.80	75	(112)	357	113	(167)	116	89	(120)	0.177	131	(182)	0.272	94	(135)
Bahrain	263	30	(46)	5.75	12	(25)	40	35	(49)	40	57	(68)	0.071	47	(76)	0.073	12	(18)
Bangladesh	298	36	(54)	8.24	61	(90)	1335	154	(223)	1254	156	(225)	0.447	156	(225)	0.660	155	(224)
Barbados	558	74	(126)	10.50	122	(176)	95	58	(94)	92	78	(105)	0.083	62	(95)	0.085	15	(23)
Belgium	400	46	(75)	8.76	73	(110)	141	72	(112)	16	51	(58)	0.038	23	(40)	0.061	9	(14)
Belize	1300	140	(206)	8.89	78	(116)	444	123	(182)	384	133	(189)	0.180	134	(186)	0.201	61	(89)
Benin	470	54	(89)	7.66	43	(69)	293	107	(160)	62	70	(86)	0.123	99	(146)	0.242	84	(118)
Brazil	478	58		7.79	49		171	82		190	112		0.098	80		0.235	76	

Sovereign / EEZ	R06	Rank		Impact	Rank		ΔR4.5	Rank		ΔR8.5	Rank		D4.5	Rank		D8.5	Rank	
Brazil	539		(117)	8.20		(89)	193		(134)	176		(147)	0.109		(131)	0.176		(76)
Trindade	92		(20)	5.24		(18)	35		(43)	280		(177)	0.031		(33)	0.607		(222)
Brunei	2161	152	(220)	9.35	93	(134)	1105	150	(219)	-684	5	(5)	0.188	137	(191)	0.498	149	(214)
Bulgaria	91	15	(19)	10.37	119	(173)	14	12	(16)	14	47	(53)	0.099	81	(116)	0.099	19	(29)
Cambodia	1229	137	(203)	8.44	64	(98)	271	103	(152)	-431	10	(10)	0.094	72	(107)	0.354	122	(175)
Cameroon	377	43	(69)	6.15	15	(32)	512	130	(191)	283	129	(179)	0.268	151	(212)	0.679	156	(225)
Canada	73	10	(13)	4.76	5	(10)	14	13	(17)	45	60	(72)	0.093	69	(104)	0.242	85	(119)
Cape Verde	547	68	(121)	10.73	128	(183)	46	38	(58)	75	76	(93)	0.028	21	(32)	0.063	10	(15)
Chile	297	35		5.90	14		42	36		92	79		0.047	30		0.171	50	
Chile	324		(60)	5.54		(22)	45		(56)	89		(103)	0.046		(49)	0.144		(57)
Easter Island	72		(12)	8.73		(109)	16		(21)	116		(119)	0.055		(60)	0.386		(186)
China	1131	131	(196)	10.82	131	(187)	484	128	(187)	622	151	(215)	0.073	51	(79)	0.386	131	(185)
Colombia	625	90	(145)	7.98	53	(79)	276	104	(154)	268	127	(175)	0.179	132	(183)	0.222	69	(101)
Comoro Islands	958	118	(181)	5.46	10	(20)	454	126	(185)	47	64	(75)	0.122	98	(145)	0.224	71	(103)
Costa Rica	455	51	(85)	4.86	6	(13)	139	70	(110)	99	83	(111)	0.073	52	(81)	0.093	16	(24)
Croatia	450	50	(83)	11.29	146	(207)	93	56	(92)	106	85	(113)	0.084	63	(97)	0.103	21	(33)
Cuba	1079	127	(191)	10.12	113	(163)	276	105	(155)	-128	24	(25)	0.079	58	(89)	0.330	117	(166)
Cyprus	86	13	(16)	10.50	123	(177)	49	40	(60)	57	67	(82)	0.249	150	(210)	0.288	103	(146)
Denmark	80	12		6.52	19		24	18		45	62		0.173	129		0.361	123	
Denmark	264		(47)	9.77		(150)	69		(77)	80		(97)	0.082		(94)	0.103		(32)
Faeroe Islands	264		(48)	12.34		(220)	110		(99)	178		(148)	0.126		(151)	0.270		(133)
Greenland	51		(7)	5.68		(24)	11		(13)	28		(60)	0.183		(189)	0.382		(183)
Disputed Chile/Peru	504	64	(106)	5.31	9	(19)	57	43	(67)	56	66	(81)	0.039	24	(41)	0.045	7	(11)
Disputed Spartly Islands	1382	141	(207)	8.69	72	(108)	1873	156	(225)	192	113	(155)	0.316	154	(219)	0.556	154	(221)
Disputed Senkaku Island	1764	148	(215)	15.69	156	(225)	1160	152	(221)	550	146	(209)	0.105	87	(126)	0.323	115	(163)
Disputed Paracel Islands	1126	130	(194)	9.46	99	(140)	923	145	(211)	692	153	(221)	0.201	140	(196)	0.446	140	(200)

Sovereign / EEZ	R06	Rank		Impact	Rank		ΔR4.5	Rank		ΔR8.5	Rank		D4.5	Rank		D8.5	Rank	
Disputed Japan/South Korea	415	47	(77)	9.01	83	(120)	153	77	(119)	219	117	(163)	0.127	103	(152)	0.210	66	(94)
Disputed Southern Kuriles	215	24	(37)	7.87	50	(76)	49	41	(61)	185	111	(153)	0.094	70	(105)	0.338	118	(168)
Djibouti	1624	144	(210)	9.65	102	(144)	57	44	(68)	-355	13	(13)	0.005	8	(8)	0.134	32	(52)
Dominica	1205	135	(201)	12.00	153	(219)	586	137	(201)	593	149	(213)	0.226	146	(205)	0.238	79	(111)
Dominican Republic	622	88	(143)	11.13	139	(199)	195	88	(135)	260	126	(174)	0.151	117	(166)	0.193	57	(84)
East Timor	3039	154	(223)	5.60	11	(23)	1466	155	(224)	-644	6	(6)	0.103	85	(124)	0.490	146	(209)
Ecuador	606	86		4.13	3		166	81		180	107		0.092	68		0.131	31	
Ecuador	758		(163)	4.77		(11)	240		(145)	294		(180)	0.124		(148)	0.196		(85)
Galapagos Islands	575		(132)	4.01		(4)	152		(117)	157		(138)	0.085		(99)	0.118		(45)
Egypt	251	28		11.36	147		98	60		173	104		0.169	128		0.282	99	
Disputed Sudan-Egypt	493		(102)	10.76		(184)	489		(189)	400		(194)	0.271		(213)	0.513		(216)
Egypt	216		(39)	11.45		(212)	41		(50)	139		(130)	0.154		(170)	0.248		(122)
El Salvador	646	96	(152)	9.40	94	(135)	2	3	(4)	-250	16	(16)	0.001	4	(4)	0.233	73	(107)
Equatorial Guinea	456	52	(86)	6.62	23	(44)	112	64	(100)	-95	29	(30)	0.041	27	(44)	0.311	111	(157)
Eritrea	1200	134	(200)	7.15	34	(58)	80	50	(84)	-226	17	(17)	0.020	17	(22)	0.178	51	(77)
Estonia	27	2	(2)	7.72	45	(72)	5	7	(8)	9	44	(50)	0.065	42	(69)	0.144	35	(56)
Fiji	1078	126	(190)	9.29	90	(131)	404	119	(175)	429	137	(197)	0.138	110	(159)	0.314	113	(158)
Finland	22	1	(1)	6.99	31	(53)	13	11	(15)	15	48	(54)	0.223	145	(203)	0.250	88	(125)
France	446	48		6.55	20		187	86		274	128		0.123	100		0.267	93	
Amsterdam Island and Saint Paul Island	340		(62)	4.72		(9)	21		(23)	70		(90)	0.012		(14)	0.096		(27)
Bassas da India	531		(114)	8.19		(88)	558		(196)	366		(187)	0.281		(216)	0.353		(174)
Clipperton Island	322		(59)	5.80		(26)	24		(24)	-7		(38)	0.026		(29)	0.095		(26)
Crozet Islands	165		(29)	6.76		(50)	29		(34)	83		(100)	0.063		(68)	0.235		(108)
France	501		(105)	10.14		(164)	162		(125)	219		(162)	0.116		(138)	0.188		(80)
French Guiana	460		(87)	9.43		(139)	155		(121)	142		(132)	0.108		(128)	0.118		(44)
French Polynesia	336		(61)	6.28		(36)	165		(126)	236		(168)	0.129		(153)	0.287		(144)

Sovereign / EEZ	R06	Rank		Impact	Rank		ΔR4.5	Rank		ΔR8.5	Rank		D4.5	Rank		D8.5	Rank	
Glorioso Islands	2463		(222)	4.32		(7)	995		(215)	277		(176)	0.180		(185)	0.273		(136)
Guadeloupe and Martinique	712		(159)	11.56		(214)	386		(172)	380		(188)	0.237		(207)	0.239		(115)
Ile Europa	505		(107)	8.25		(91)	224		(140)	390		(190)	0.112		(134)	0.287		(145)
Ile Tromelin	364		(66)	5.89		(28)	183		(130)	633		(216)	0.074		(83)	0.425		(197)
Juan de Nova Island	636		(148)	6.30		(37)	979		(214)	660		(219)	0.302		(217)	0.459		(204)
Kerguelen Islands	231		(42)	6.55		(40)	41		(52)	114		(117)	0.100		(119)	0.247		(121)
Mayotte	897		(178)	5.01		(16)	277		(156)	-31		(34)	0.099		(117)	0.227		(105)
New Caledonia	967		(183)	5.91		(31)	373		(170)	642		(218)	0.131		(155)	0.255		(126)
Réunion	528		(112)	7.22		(59)	173		(128)	390		(191)	0.371		(221)	0.493		(212)
Saint Pierre and Miquelon	276		(51)	11.90		(217)	84		(89)	199		(157)	0.068		(72)	0.270		(134)
Wallis and Futuna	401		(76)	9.79		(154)	272		(153)	16		(56)	0.120		(141)	0.366		(176)
Gabon	491	62	(101)	6.59	22	(42)	237	95	(144)	-71	30	(31)	0.108	89	(130)	0.346	120	(170)
Gambia	625	89	(144)	11.03	136	(196)	96	59	(96)	136	94	(128)	0.072	49	(78)	0.168	48	(71)
Georgia	62	9	(11)	10.22	116	(168)	26	20	(26)	26	52	(59)	0.223	144	(202)	0.223	70	(102)
Germany	187	22	(34)	8.55	69	(104)	31	26	(36)	47	65	(77)	0.043	28	(45)	0.076	14	(20)
Ghana	579	79	(133)	8.51	68	(102)	31	27	(37)	-134	23	(24)	0.006	10	(10)	0.154	37	(60)
Greece	203	23	(36)	11.61	150	(215)	38	33	(47)	73	75	(92)	0.112	91	(133)	0.235	75	(109)
Grenada	1143	132	(197)	10.90	133	(192)	278	106	(158)	252	123	(171)	0.131	105	(154)	0.142	34	(55)
Guatemala	652	97	(153)	7.79	48	(75)	15	14	(18)	-310	15	(15)	0.002	6	(6)	0.309	108	(154)
Guinea	629	91	(146)	9.22	88	(129)	162	80	(124)	9	43	(49)	0.070	45	(74)	0.165	46	(69)
Guinea Bissau	665	98	(155)	9.09	86	(124)	117	65	(102)	4	42	(48)	0.057	38	(63)	0.165	45	(68)
Guyana	785	108	(167)	9.19	87	(127)	149	76	(116)	162	101	(143)	0.060	39	(64)	0.096	18	(28)
Haiti	665	99	(156)	10.76	129	(185)	157	78	(122)	59	68	(83)	0.095	75	(110)	0.180	53	(79)
Honduras	1033	124	(188)	8.88	77	(115)	243	97	(147)	149	96	(134)	0.094	73	(108)	0.159	41	(64)
Iceland	224	26	(40)	11.22	143	(203)	51	42	(64)	99	82	(110)	0.068	44	(73)	0.180	52	(78)
India	807	111		8.93	79		840	144		410	135		0.212	143		0.38	129	

Sovereign / EEZ	R06	Rank		Impact	Rank		ΔR4.5	Rank		ΔR8.5	Rank		D4.5	Rank		D8.5	Rank	
Andaman and Nicobar	830		(174)	9.11		(125)	971		(213)	250		(170)	0.183		(188)	0.453		(203)
India	797		(171)	8.85		(114)	784		(209)	478		(203)	0.224		(204)	0.349		(172)
Indonesia	2249	153	(221)	6.66	24	(45)	796	143	(210)	-842	4	(4)	0.118	94	(139)	0.453	141	(202)
Iran	573	76	(129)	7.47	38	(63)	99	61	(97)	-310	14	(14)	0.050	32	(55)	0.487	144	(207)
Ireland	470	55	(90)	12.35	154	(221)	141	73	(113)	205	116	(161)	0.097	79	(114)	0.164	44	(67)
Israel	106	17	(23)	10.25	117	(170)	16	16	(20)	16	50	(57)	0.151	115	(164)	0.151	36	(59)
Italy	346	39	(63)	10.42	121	(175)	146	74	(114)	160	100	(141)	0.195	139	(195)	0.235	77	(110)
Ivory Coast	557	73	(125)	9.07	85	(122)	93	55	(91)	-69	31	(32)	0.033	22	(36)	0.190	56	(82)
Jamaica	812	113	(173)	10.34	118	(172)	229	93	(142)	155	98	(136)	0.120	96	(142)	0.239	80	(113)
Japan	774	106	(165)	10.56	125	(179)	184	84	(131)	235	121	(166)	0.054	36	(59)	0.200	60	(88)
Joint Development Australia - East Timor	3265	155	(224)	4.88	7	(14)	62	48	(74)	-1873	2	(2)	0.012	12	(13)	0.419	136	(194)
Joint Regime Colombia - Jamaica	731	102	(187)	9.80	107	(222)	578	136	(105)	999	155	(222)	0.181	135	(187)	0.418	135	(193)
Joint Regime Japan - Korea	977	123	(160)	12.88	155	(155)	120	67	(199)	843	154	(224)	0.015	14	(16)	0.282	100	(140)
Joint Regime Nigeria - Sao Tome and Principe	389	44	(74)	8.02	54	(81)	17	17	(22)	-138	22	(23)	0.002	5	(5)	0.249	87	(123)
Kenya	1108	128	(192)	7.41	37	(62)	506	129	(190)	580	147	(211)	0.088	66	(102)	0.239	81	(114)
Kiribati	547	70		6.87	28		246	100		65	72		0.102	84		0.236	78	
Kiribati	867		(176)	9.17		(126)	486		(188)	-14		(37)	0.125		(150)	0.295		(148)
Line Group	388		(72)	5.03		(17)	114		(101)	104		(112)	0.087		(100)	0.190		(83)
Phoenix Group	448		(82)	7.61		(67)	197		(137)	89		(102)	0.102		(122)	0.250		(124)
Kuwait	286	34	(53)	8.03	56	(83)	29	24	(30)	113	87	(115)	0.154	120	(171)	0.102	20	(31)
Latvia	30	3	(3)	10.37	120	(174)	3	5	(5)	3	39	(45)	0.043	29	(46)	0.043	6	(10)
Lebanon	123	18	(25)	11.20	142	(202)	60	46	(72)	60	69	(84)	0.242	149	(209)	0.242	83	(117)
Liberia	552	72	(123)	9.43	97	(138)	94	57	(93)	-100	27	(28)	0.024	19	(25)	0.202	62	(91)
Libya	170	20	(31)	10.91	135	(195)	61	47	(73)	76	77	(94)	0.168	127	(178)	0.198	59	(87)
Lithuania	35	4	(4)	9.32	91	(132)	0	1	(1)	0	37	(43)	0.000	1	(1)	0.000	1	(1)
Madagascar	1049	125	(189)	7.48	39	(64)	520	133	(194)	514	144	(206)	0.150	114	(163)	0.278	98	(138)

Sovereign / EEZ	R06	Rank		Impact	Rank		ΔR4.5	Rank		ΔR8.5	Rank		D4.5	Rank		D8.5	Rank	
Malaysia	2100	151	(219)	10.19	115	(166)	303	108	(161)	-995	3	(3)	0.065	43	(70)	0.391	132	(187)
Maldives	937	116	(180)	8.32	63	(95)	605	138	(202)	-61	32	(33)	0.161	123	(174)	0.340	119	(169)
Malta	216	25	(38)	10.05	111	(160)	30	25	(35)	35	53	(62)	0.095	74	(109)	0.109	25	(39)
Marshall Islands	677	100	(157)	8.49	67	(101)	783	142	(208)	236	122	(167)	0.278	152	(215)	0.489	145	(208)
Mauritania	284	33	(52)	10.70	127	(181)	58	45	(70)	156	99	(137)	0.061	41	(67)	0.219	68	(100)
Mauritius	481	59	(96)	6.44	18	(39)	386	117	(173)	464	141	(202)	0.179	133	(184)	0.301	107	(152)
Mexico	630	92	(147)	7.12	33	(56)	199	90	(138)	71	74	(91)	0.071	48	(77)	0.240	82	(116)
Micronesia	605	84	(141)	7.34	36	(61)	361	115	(169)	-99	28	(29)	0.151	116	(165)	0.385	130	(184)
Montenegro	348	40	(64)	11.42	148	(210)	205	91	(139)	180	108	(150)	0.205	142	(198)	0.205	63	(92)
Morocco	606	85		10.00	110		117	66		162	102		0.076	56		0.126	30	
Morocco	658		(154)	10.24		(169)	153		(118)	165		(144)	0.107		(127)	0.120		(46)
Western Sahara	556		(124)	9.77		(152)	83		(87)	160		(142)	0.047		(50)	0.131		(51)
Mozambique	1273	139	(205)	6.57	21	(41)	565	135	(197)	540	145	(207)	0.176	130	(181)	0.300	106	(151)
Myanmar	797	109	(169)	7.49	40	(65)	1012	147	(216)	581	148	(212)	0.310	153	(218)	0.476	142	(205)
Namibia	472	56	(91)	8.26	62	(92)	35	30	(44)	97	81	(108)	0.025	20	(28)	0.107	23	(37)
Nauru	602	83	(140)	9.78	106	(153)	246	98	(148)	-139	21	(22)	0.080	59	(91)	0.264	91	(131)
Netherlands	743	104		9.63	100		107	63		113	86		0.087	65		0.111	26	
Aruba	543		(118)	10.82		(188)	290		(159)	282		(178)	0.216		(201)	0.219		(99)
Bonaire	1150		(198)	11.27		(206)	41		(51)	38		(64)	0.036		(38)	0.039		(8)
Curaçao	1821		(216)	10.85		(191)	32		(38)	42		(69)	0.006		(11)	0.015		(5)
Netherlands	307		(55)	8.27		(93)	75		(81)	92		(106)	0.084		(98)	0.129		(49)
Saba	1655		(211)	10.22		(167)	121		(106)	114		(118)	0.035		(37)	0.037		(7)
New Zealand	397	45		6.80	27		88	53		150	97		0.070	46		0.234	74	
Cook Islands	255		(44)	8.69		(107)	84		(88)	82		(99)	0.103		(123)	0.324		(164)
New Zealand	478		(94)	5.50		(21)	95		(95)	191		(154)	0.056		(61)	0.172		(73)
Niue	167		(30)	9.69		(146)	73		(79)	338		(185)	0.097		(115)	0.490		(210)

Sovereign / EEZ	R06	Rank		Impact	Rank		ΔR4.5	Rank		ΔR8.5	Rank		D4.5	Rank		D8.5	Rank	
Tokelau	420		(79)	9.69		(148)	32		(39)	-152		(21)	0.031		(34)	0.258		(127)
Nicaragua	1109	129	(193)	7.66	44	(70)	317	111	(164)	203	115	(159)	0.097	78	(113)	0.157	40	(63)
Nigeria	590	82	(136)	8.82	76	(113)	148	75	(115)	-105	26	(27)	0.054	35	(57)	0.291	104	(147)
North Korea	271	31	(49)	8.67	71	(106)	85	52	(90)	255	125	(173)	0.096	76	(111)	0.323	114	(162)
Norway	93	16		7.02	32		36	31		63	71		0.135	107		0.312	112	
Bouvet Island	86		(15)	3.13		(2)	3		(6)	68		(89)	0.016		(17)	0.315		(160)
Jan Mayen	61		(10)	7.11		(55)	28		(27)	55		(80)	0.121		(143)	0.336		(167)
Norway	100		(22)	8.01		(80)	46		(57)	63		(87)	0.169		(179)	0.306		(153)
Oman	584	81	(135)	9.69	104	(147)	389	118	(174)	412	136	(196)	0.166	125	(176)	0.258	89	(128)
Pakistan	467	53	(88)	8.80	74	(111)	385	116	(171)	638	152	(217)	0.203	141	(197)	0.369	125	(178)
Palau	638	95	(151)	7.25	35	(60)	1051	148	(217)	36	54	(63)	0.239	148	(208)	0.501	150	(215)
Panama	637	94	(150)	8.03	57	(84)	268	101	(150)	180	109	(151)	0.152	118	(168)	0.189	55	(81)
Papua New Guinea	1756	146	(213)	6.92	30	(52)	936	146	(212)	-376	12	(12)	0.137	109	(158)	0.432	139	(198)
Peru	487	60	(98)	4.91	8	(15)	159	79	(123)	179	106	(149)	0.113	92	(135)	0.161	42	(65)
Philippines	1977	150	(218)	8.94	80	(117)	1322	153	(222)	-466	8	(8)	0.229	147	(206)	0.530	152	(218)
Poland	36	5	(5)	11.23	144	(204)	3	6	(7)	3	40	(46)	0.041	26	(43)	0.041	5	(9)
Portugal	520	65		9.86	109		82	51		137	95		0.050	33		0.112	27	
Azores	528		(111)	10.12		(162)	74		(80)	123		(124)	0.045		(48)	0.103		(34)
Madeira	451		(84)	10.31		(171)	62		(75)	90		(104)	0.045		(47)	0.084		(21)
Portugal	591		(137)	8.51		(103)	132		(108)	241		(169)	0.073		(80)	0.173		(74)
Qatar	256	29	(45)	6.73	26	(48)	39	34	(48)	-161	20	(20)	0.018	15	(19)	0.526	151	(217)
République du Congo	274	32	(50)	7.93	52	(78)	407	121	(177)	307	130	(181)	0.166	126	(177)	0.166	47	(70)
Romania	89	14	(18)	9.63	101	(143)	38	32	(45)	38	55	(66)	0.153	119	(169)	0.265	92	(132)
Russia	46	6	(6)	4.24	4	(5)	25	19	(25)	44	59	(71)	0.104	86	(125)	0.311	109	(155)
Saint Kitts and Nevis	1547	143	(209)	10.84	132	(190)	125	68	(107)	232	120	(165)	0.020	16	(21)	0.073	13	(19)
Saint Lucia	968	120	(184)	11.96	152	(218)	8	9	(10)	-5	35	(39)	0.004	7	(7)	0.011	4	(4)

Sovereign / EEZ	R06	Rank		Impact	Rank		ΔR4.5	Rank		ΔR8.5	Rank		D4.5	Rank		D8.5	Rank	
Saint Vincent and the Grenadines	977	122	(186)	11.08	138	(198)	0	2	(2)	-19	34	(36)	0.000	2	(2)	0.006	3	(3)
Samoa	636	93	(149)	10.09	112	(161)	406	120	(176)	97	80	(107)	0.190	138	(192)	0.398	133	(189)
Sao Tome and Principe	490	61	(100)	6.90	29	(51)	11	10	(12)	-219	18	(18)	0.006	11	(12)	0.287	102	(143)
Saudi Arabia	575	78	(131)	8.97	82	(119)	241	96	(146)	117	91	(122)	0.137	108	(157)	0.376	127	(181)
Senegal	563	75	(127)	10.82	130	(186)	70	49	(78)	170	103	(145)	0.040	25	(42)	0.163	43	(66)
Seychelles	809	112	(172)	6.16	16	(33)	470	127	(186)	65	73	(88)	0.121	97	(144)	0.258	90	(129)
Sierra Leone	527	66	(109)	9.77	105	(151)	33	28	(40)	-107	25	(26)	0.014	13	(15)	0.157	39	(62)
Solomon Islands	1178	133	(199)	9.42	96	(137)	605	139	(203)	-398	11	(11)	0.108	88	(129)	0.406	134	(192)
Somalia	960	119	(182)	8.06	58	(85)	515	132	(193)	452	139	(200)	0.161	124	(175)	0.225	72	(104)
South Africa	448	49		8.06	59		130	69		182	110		0.075	54		0.184	54	
Prince Edward Islands	201		(35)	5.89		(29)	49		(62)	140		(131)	0.070		(75)	0.298		(149)
South Africa	564		(128)	9.07		(123)	167		(127)	202		(158)	0.078		(87)	0.130		(50)
South Korea	534	67	(116)	11.04	137	(197)	186	85	(132)	622	150	(214)	0.074	53	(82)	0.329	116	(165)
Spain	548	71		9.44	98		91	54		125	92		0.073	50		0.114	29	
Canary Islands	596		(138)	10.72		(182)	44		(54)	60		(85)	0.025		(27)	0.047		(12)
Spain	506		(108)	8.31		(94)	133		(109)	183		(152)	0.115		(137)	0.174		(75)
Sri Lanka	851	114	(175)	11.54	149	(213)	323	112	(165)	4	41	(47)	0.087	64	(101)	0.273	95	(137)
Sudan	699	101	(158)	9.34	92	(133)	312	110	(163)	114	88	(116)	0.161	122	(173)	0.484	143	(206)
Suriname	772	105	(164)	9.67	103	(145)	270	102	(151)	255	124	(172)	0.100	82	(120)	0.108	24	(38)
Sweden	54	7	(8)	9.81	108	(156)	15	15	(19)	16	49	(55)	0.124	101	(147)	0.142	33	(54)
Syria	186	21	(33)	11.25	145	(205)	2	4	(3)	2	38	(44)	0.005	9	(9)	0.005	2	(2)
Taiwan	1757	147	(214)	11.66	151	(216)	1056	149	(218)	503	142	(204)	0.124	102	(149)	0.423	138	(196)
Tanzania	1261	138	(204)	5.85	13	(27)	449	125	(184)	10	46	(52)	0.051	34	(56)	0.154	38	(61)
Thailand	1487	142	(208)	7.92	51	(77)	442	122	(180)	-432	9	(9)	0.157	121	(172)	0.421	137	(195)
Togo	742	103	(162)	8.18	60	(87)	446	124	(183)	451	138	(199)	0.144	112	(161)	0.245	86	(120)
Tonga	613	87	(142)	9.02	84	(121)	233	94	(143)	453	140	(201)	0.111	90	(132)	0.298	105	(150)

Sovereign / EEZ	R06	Rank		Impact	Rank		ΔR4.5	Rank		ΔR8.5	Rank		D4.5	Rank		D8.5	Rank	
Trinidad and Tobago	797	110	(170)	10.53	124	(178)	196	89	(136)	175	105	(146)	0.100	83	(121)	0.113	28	(42)
Tunisia	547	69	(122)	10.68	126	(180)	29	22	(29)	45	61	(73)	0.021	18	(23)	0.052	8	(13)
Turkey	152	19	(27)	11.19	141	(201)	34	29	(42)	43	58	(70)	0.082	61	(93)	0.105	22	(36)
Tuvalu	498	63	(104)	9.41	95	(136)	246	99	(149)	-176	19	(19)	0.096	77	(112)	0.380	128	(182)
Ukraine	75	11	(14)	9.22	89	(130)	29	21	(28)	39	56	(67)	0.141	111	(160)	0.209	65	(93)
United Arab Emirates	581	80	(134)	7.74	46	(73)	360	114	(168)	-25	33	(35)	0.050	31	(54)	0.555	153	(220)
United Kingdom	336	38		7.65	42		103	62		104	84		0.078	57		0.207	64	
Anguilla	485		(97)	11.45		(211)	571		(198)	569		(210)	0.400		(223)	0.401		(190)
Ascension	489		(99)	6.24		(35)	59		(71)	0		(42)	0.048		(51)	0.111		(40)
Bermuda	416		(78)	9.82		(157)	58		(69)	79		(96)	0.050		(53)	0.084		(22)
British Indian Ocean Territory	792		(168)	8.34		(96)	416		(179)	87		(101)	0.172		(180)	0.317		(161)
British Virgin Islands	495		(103)	11.31		(208)	415		(178)	410		(195)	0.375		(222)	0.376		(180)
Cayman Islands	528		(113)	9.82		(158)	65		(76)	160		(140)	0.024		(26)	0.285		(142)
Falkland Islands	225		(41)	7.14		(57)	38		(46)	50		(78)	0.065		(71)	0.100		(30)
Guernsey	534		(115)	14.54		(224)	56		(65)	38		(65)	0.049		(52)	0.064		(16)
Montserrat	899		(179)	10.83		(189)	34		(41)	29		(61)	0.018		(20)	0.020		(6)
Pitcairn	86		(17)	7.57		(66)	29		(32)	122		(123)	0.076		(85)	0.391		(188)
Saint Helena	426		(80)	5.90		(30)	45		(55)	106		(114)	0.027		(31)	0.112		(41)
South Georgia and the South Sandwich Islands	96		(21)	4.25		(6)	9		(11)	47		(76)	0.032		(35)	0.214		(96)
Tristan da Cunha	381		(71)	6.68		(47)	29		(33)	97		(109)	0.016		(18)	0.117		(43)
Turks and Caicos Islands	389		(73)	10.91		(194)	578		(200)	548		(208)	0.439		(224)	0.447		(201)
United Kingdom	429		(81)	13.57		(223)	108		(98)	153		(135)	0.084		(96)	0.140		(53)
United States	367	42		8.66	70		179	83		232	119		0.128	104		0.276	96	
Alaska	157		(28)	8.09		(86)	79		(83)	142		(133)	0.152		(167)	0.314		(159)
American Samoa	318		(58)	9.89		(159)	277		(157)	128		(126)	0.256		(211)	0.432		(199)
Hawaii	479		(95)	9.48		(141)	117		(103)	159		(139)	0.079		(90)	0.146		(58)

Sovereign / EEZ	R06	Rank		Impact	Rank		ΔR4.5	Rank		ΔR8.5	Rank		D4.5	Rank		D8.5	Rank	
Howland Island and Baker Island	527		(110)	7.72		(71)	443		(181)	392		(193)	0.191		(193)	0.239		(112)
Jarvis Island	373		(68)	4.70		(8)	57		(66)	78		(95)	0.061		(65)	0.104		(35)
Johnston Atoll	308		(56)	9.48		(142)	81		(86)	139		(129)	0.077		(86)	0.201		(90)
Northern Mariana Islands and Guam	372		(67)	9.21		(128)	638		(206)	687		(220)	0.277		(214)	0.531		(219)
Palmyra Atoll	473		(92)	6.41		(38)	119		(104)	-2		(41)	0.054		(58)	0.128		(48)
Puerto Rico and Virgin Islands of the United States	742		(161)	11.35		(209)	310		(162)	316		(182)	0.193		(194)	0.213		(95)
United States	546		(119)	8.67		(105)	180		(129)	196		(156)	0.079		(88)	0.228		(106)
Wake Island	182		(32)	9.73		(149)	154		(120)	908		(223)	0.100		(118)	0.645		(223)
Uruguay	313	37	(57)	8.02	55	(82)	228	92	(141)	391	134	(192)	0.188	136	(190)	0.353	121	(173)
Vanuatu	1211	136	(202)	8.46	65	(99)	613	140	(204)	346	132	(186)	0.115	93	(136)	0.285	101	(141)
Venezuela	889	115	(177)	10.17	114	(165)	141	71	(111)	136	93	(127)	0.061	40	(66)	0.067	11	(17)
Vietnam	1882	149	(217)	8.48	66	(100)	755	141	(207)	231	118	(164)	0.134	106	(156)	0.375	126	(179)
Yemen	782	107	(166)	8.97	81	(118)	529	134	(195)	329	131	(183)	0.148	113	(162)	0.168	49	(72)